

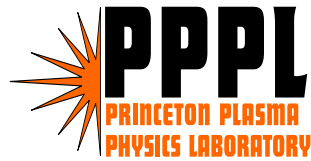
# Mode Particle Resonance in toroidal fusion devices

**Roscoe White**

*Plasma Physics Laboratory, Princeton University*

June 2011

Supported by US DoE

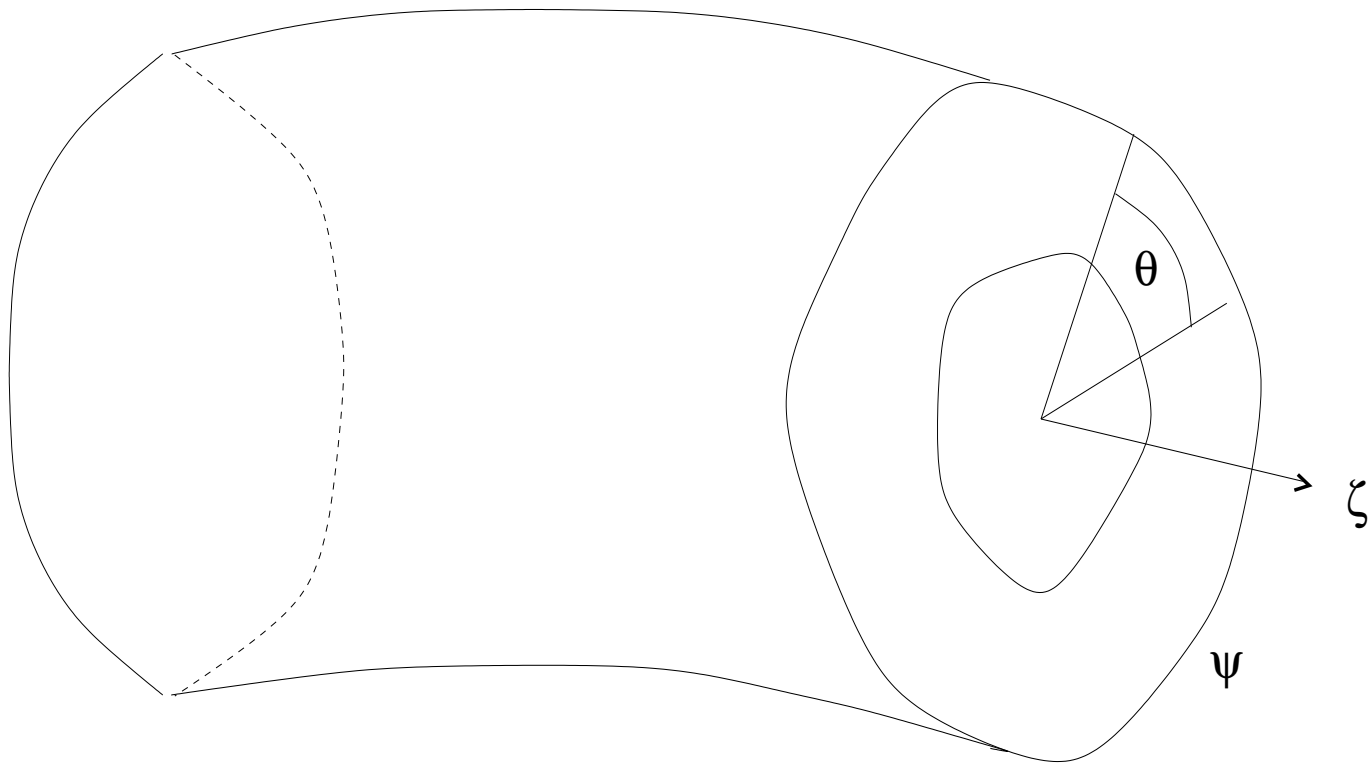


# Outline

- Motivation
- Mode Particle Resonance, Kinetic Poincaré Plots
- Phase mixing and Landau Damping
- Stochastic Transport
- Orbit Classification
- Phase Vector Rotation determination of broken KAM surfaces
- Evolution of a particle distribution using the broken KAM domains
- A single mode multi-resonance avalanche
- TAE modes in DIII-D shot 122117

## Motivation

- Observations on DIII-D, on NSTX and other tokamaks show a strong modification of the high energy beam particle distribution from that given by beam deposition physics when MHD perturbations are present
- In DIII-D toroidal Alfvén modes and reversed shear Alfvén modes are present, but with very low amplitude,  $dB/B = 2 \times 10^{-4}$ .  
The high energy beam profile is flattened significantly.
- The same could occur by Alfvén mode modification of the alpha profile in ITER. Stochastic ripple loss is very sensitive to the alpha density profile and thus low amplitude modes could cause significant loss.
- Distribution changes can only be caused by mode-particle resonance. Without resonance only periodic reversible changes occur. Resonances produce islands in the phase space of the particle orbits which locally flatten the distribution. Overlapping islands produce large scale stochastic transport.



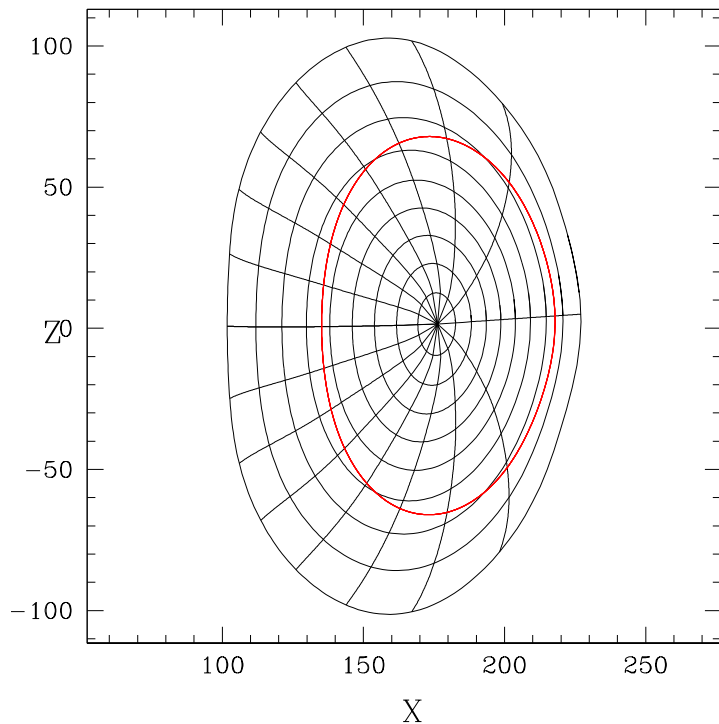
Tokamak or Stellarator equilibrium

General Toroidal coordinates,

toroidal flux label  $\psi$  or poloidal flux label  $\psi_p$  (minor radius),

poloidal angle  $\theta$  and toroidal angle  $\zeta$ .

Quasilinear diffusion models have a major problem in being able to accurately locate resonances and island widths.



High energy particle orbits have significant drift, moving across flux surfaces.  
 Location and number of resonances for a given perturbation is nontrivial.  
 Perturbation amplitude can be a highly localized function of flux surface  $f(\psi)$ .  
 Normal procedure of using mode amplitude to calculate island width is unclear.

Fourier decompose perturbation  $\delta B \sim \sum \sin(n\zeta - m\theta - \omega t)$

Conventional Wisdom: perturbation  $\frac{m}{n}$  couples to drift- resonance  $\frac{m \pm 1}{n}$

Straight field line Boozer coordinates  $\psi_p, \theta, \zeta$ , with  $d\zeta/d\theta = q(\psi)$

Normalized parallel velocity  $\rho_{\parallel} = v_{\parallel}/B$

Covariant representation of  $\vec{B}$  —  $\vec{B} = g(\psi_p)\nabla\zeta + I(\psi_p)\nabla\theta + \delta(\psi_p, \theta)\nabla\psi_p$

Canonical momentum, toroidal flux  $\psi$ ,  $d\psi/d\psi_p = q$

$$P_{\zeta} = g\rho_{\parallel} - \psi_p, \quad P_{\theta} = \psi + \rho_{\parallel}I,$$

Hamiltonian  $H = \rho_{\parallel}^2 B^2/2 + \mu B + \Phi$ , (See ITER summer school lectures, R. B. White, Aix 2009)

$$\begin{aligned} \dot{\theta} &= \frac{\partial H}{\partial P_{\theta}} & \dot{P}_{\theta} &= -\frac{\partial H}{\partial \theta} \\ \dot{\zeta} &= \frac{\partial H}{\partial P_{\zeta}} & \dot{P}_{\zeta} &= -\frac{\partial H}{\partial \zeta}. \end{aligned}$$

Perturbation  $\delta\vec{B} = \nabla \times \alpha\vec{B}$  and  $\alpha = \sum_{m,n} \alpha_{m,n}(\psi_p) \sin(n\zeta - m\theta - \omega_n t)$ ,  $\Phi$   
Mode frequency much less than cyclotron frequency, so  $\mu$  is constant

## Resonance Determination - Kinetic Poincaré Plot

Single  $n$ , Hamiltonian a function of the combination  $n\zeta - \omega t$ ,

then from  $\dot{P}_\zeta = -\frac{\partial H}{\partial \zeta}$  and  $\frac{dE}{dt} = \frac{\partial H}{\partial t}$ , with  $P_\zeta = g\rho_{||} - \psi_p$

Fixed  $n, \mu$  we have  $E - P_\zeta\omega/n = \text{constant}$  in time - Energy in mode frame

Kinetic Poincaré plot - plot of positions of orbits in the  $P_\zeta, \theta$  plane

at times when  $n\zeta - \omega t = 2\pi k$ ,  $k$  integer

All particles having the same value of  $E - P_\zeta\omega/n$  and  $\mu$

This plot shows mode-particle resonances along  $E - P_\zeta\omega/n = \text{constant}$

**Can make the Poincaré plot in the  $P_\zeta, \theta$  or in the  $\psi_p, \theta$  plane.**

Given  $P_\zeta, \theta$ ,  $E$  is determined, so also  $\rho_{||}$  and  $\psi_p$ .

$P_\zeta$  is constant without perturbation, but perturbation is function of  $\psi_p$ .

## Analytic Resonance Determination

Fixed  $\mu$ ,  $n$ , and  $E - P_\zeta \omega/n$

A kinetic Poincaré point in the  $P_\zeta, \theta$  plane occurs when  $n\zeta - \omega_n t = 2\pi k$ .

Also require  $\Delta\theta = 2\pi l/m'$  between successive points with  $l$  integer. Here  $m'$  is the number of islands in a poloidal cross section Poincaré plot.

The helicity of the resonance is then

$$h(P_\zeta, E, \mu) = \frac{\langle \dot{\zeta} \rangle - \omega_n/n}{\langle \dot{\theta} \rangle} = \frac{m'}{nl}, \quad h \simeq q \left[ 1 - \frac{\omega_n R}{nv_{\parallel}} \right].$$

$h$  does not involve the poloidal mode number  $m$ , or the perturbation.

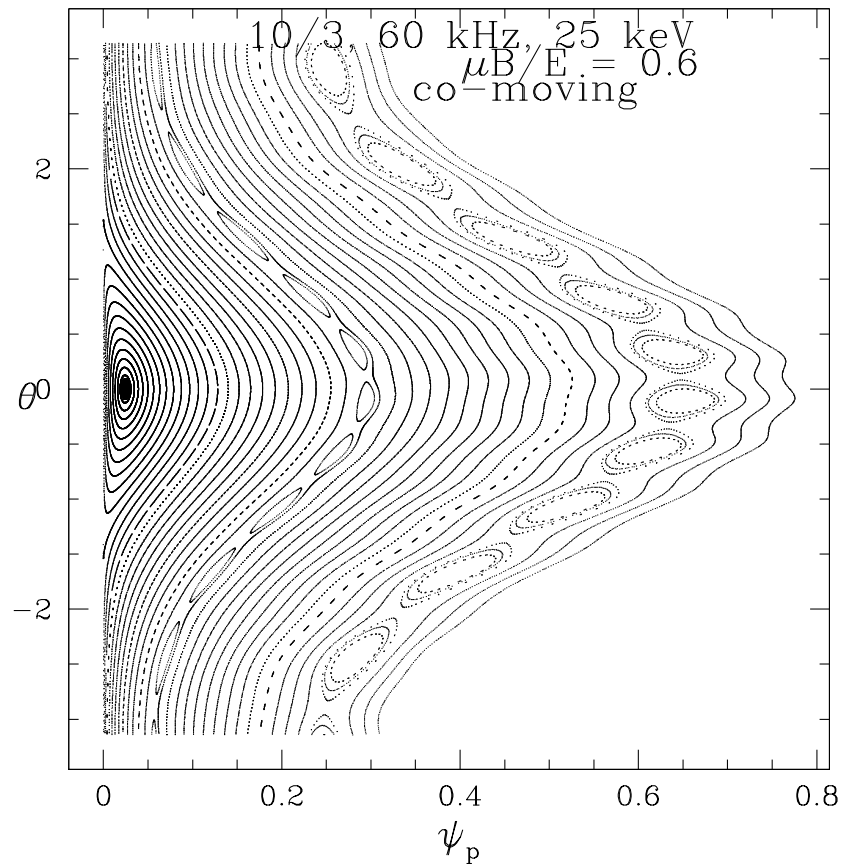
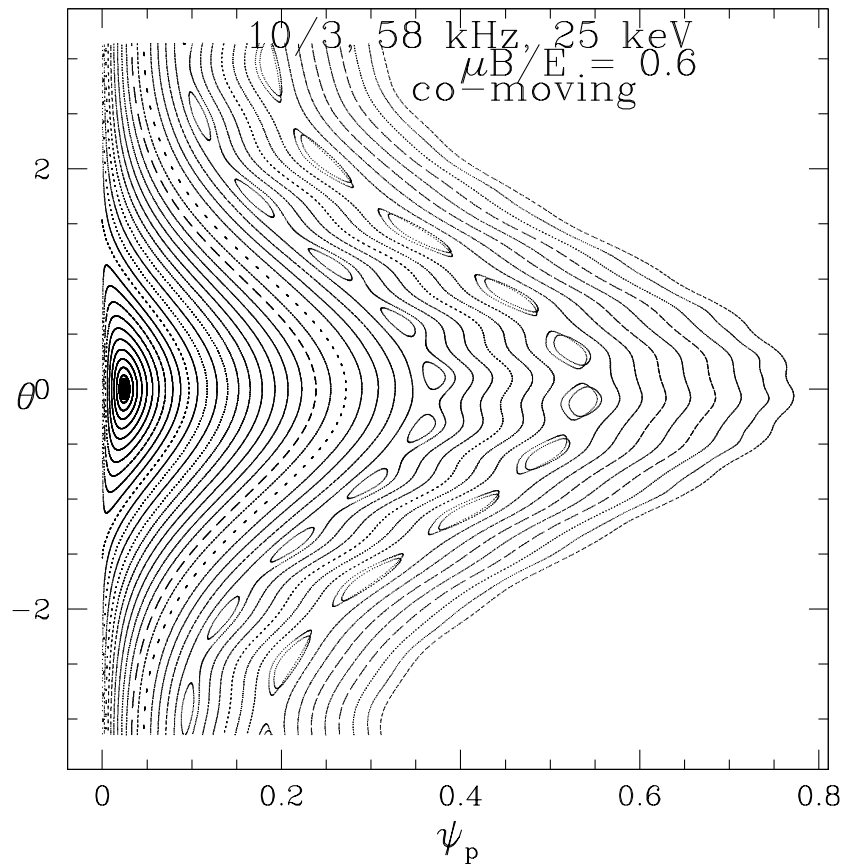
Resonance - there must exist integers  $m', l$  such that  $h$  is rational.

**Necessary but not sufficient condition for an island to appear.**

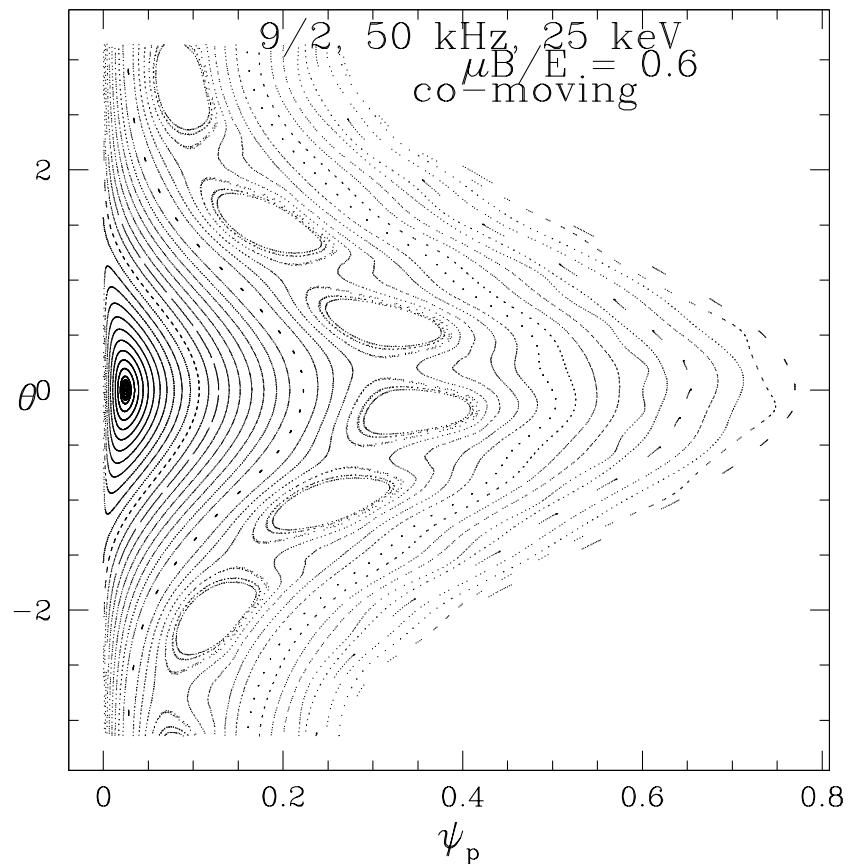
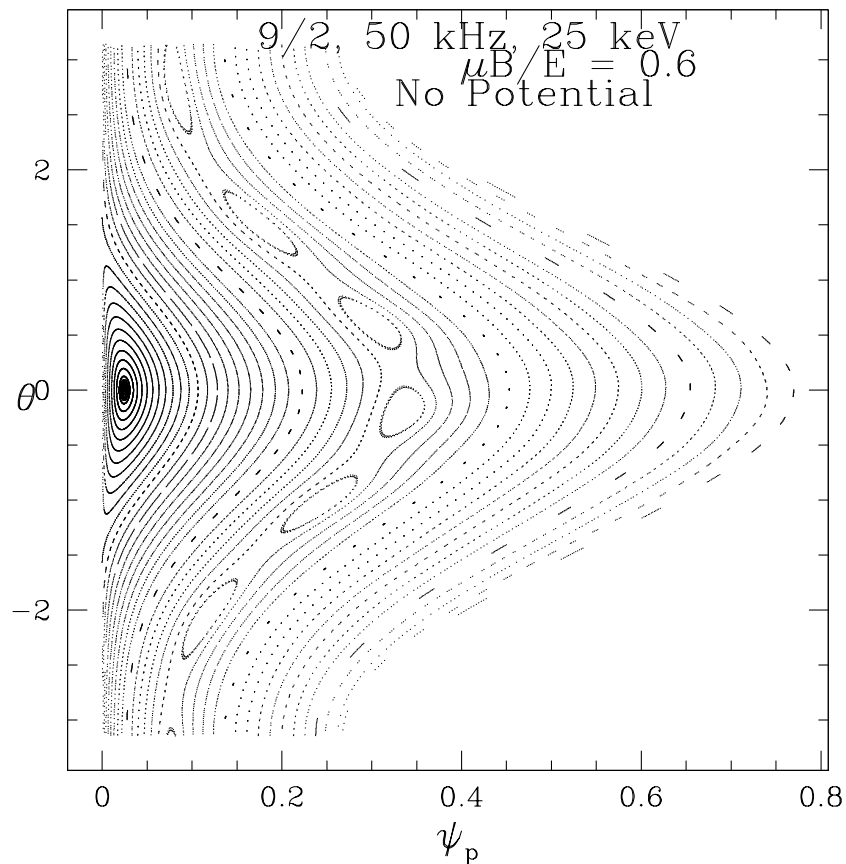
**Perturbation must be large enough to induce variations in  $P_\zeta$ .**

Normally  $m'$  not far removed from  $m$  values present in  $\delta\vec{B}$ .

Convention wisdom is that  $m' = m \pm 1$

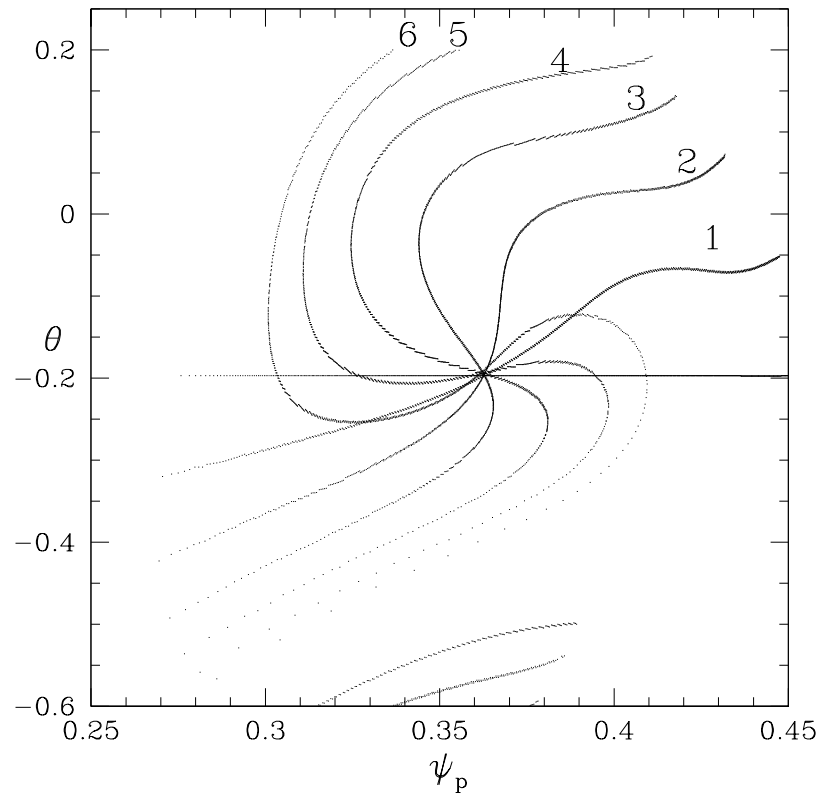
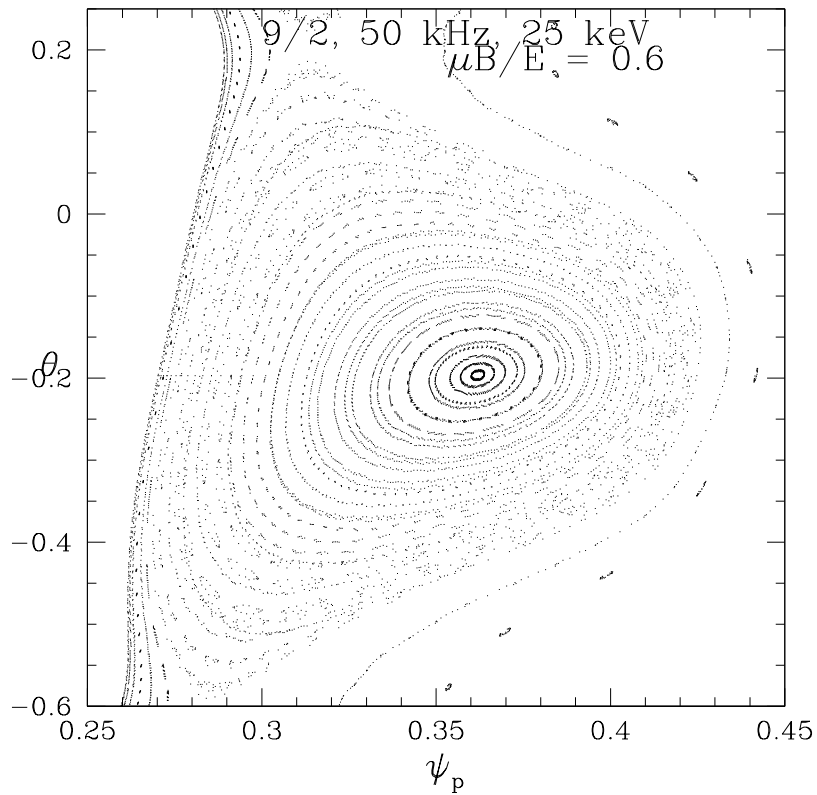


Kinetic Poincaré for co-moving beam for a 10/3 mode, 58 and 60 kHz.  
 Large  $\cos(\theta)$  motion is particle drift  
 This is a reversed shear  $q$  profile, with the minimum  $q$  value between the resonances  
 Larger  $\omega$  means larger  $q$  for resonance, they move apart.



Kinetic Poincaré plots for mode  $m/n = 9/2$ , showing the effect of the potential on 23 Kev beam particles for a 50 kHz mode.  $m' = 6!!$ . Representation  $\delta\vec{B} = \nabla \times \alpha\vec{B}$  gives nonzero  $E_{\parallel}$  from  $dB/dt$ . But ideal mode has  $E_{\parallel} = 0$  so this must be cancelled by  $\Phi$ . Setting  $E_{\parallel} = 0$  forms a larger resonance island. Is this general?

## Landau Phase Mixing



Kinetic Poincaré plot of a TAE resonance island, and a plot showing the time evolution of points placed initially at  $\theta = -0.2$ , for a period of 0.34 msec. Near the O-point a full period is approximately 0.5 msec. Original Kolmogorov Arnold Moser (KAM) surfaces broken by island

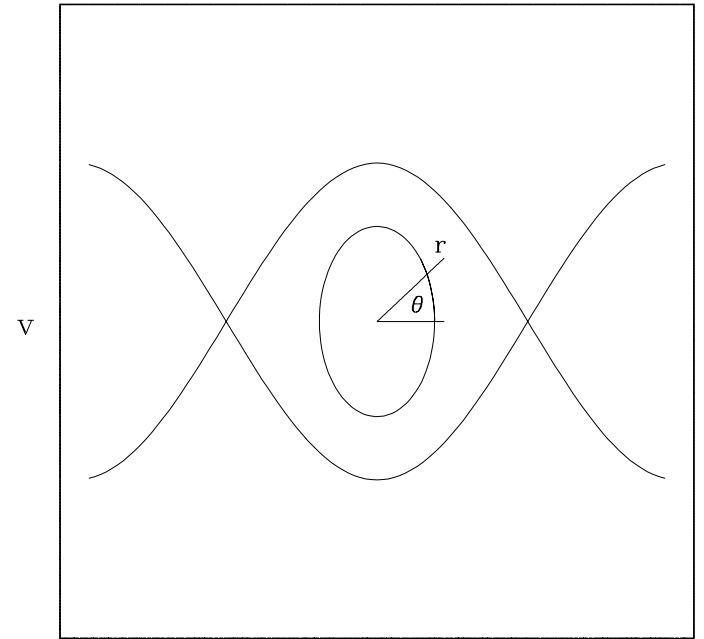
## Nonlinear Landau Damping

Model Phase mixing due to an island

Introduce at  $t = 0$  a gradient in particle density in velocity space,  $n(v, q) = 1 + \delta v = 1 + \delta r \sin \theta_0$

$\delta =$  inverse scale length for the velocity gradient,  $v_r =$  velocity at x-point

In time the particles rotate about the O-point as seen with  $\theta(t) = \theta_0 + \omega(r)t$ .



Average energy of particles trapped in the island  $\langle E \rangle \simeq \int_0^q r dr d\theta n v^2$

$$\langle v^2(t) \rangle = \frac{1}{\pi V^2} \int_0^V r dr \int_0^{2\pi} d\theta [v_r + r \sin \theta]^2 [1 + \delta r \sin \theta \cos(\omega t) - \delta r \cos \theta \sin(\omega t)]$$

where  $V$  is the island half width in velocity space.  $\theta$  integration gives

$$\langle v^2(t) \rangle = v_r^2 + \frac{V^2}{4} + \frac{\delta v_r}{V^2} \int_0^V r^3 dr \cos(\omega t)$$

Initial mean energy  $\langle v^2(t) \rangle = v_r^2 + V^2/4 + \delta v_r V^2/4$ .

Approximate the frequency of rotation about the O-point,

$$\omega(r) = \omega_0(1 - r^2/V^2).$$

Then

$$\langle v^2(t) \rangle = v_r^2 + \frac{V^2}{4} + \frac{\delta v_r^2}{2\omega_0 t} \left[ \sin \omega_0 t + \frac{(\cos \omega_0 t - 1)}{\omega_0 t} \right],$$

and for small  $t$  we have

$$\langle v^2(t) \rangle = v_r^2 + \frac{V^2}{4} + \delta v_r V^2 \left[ 1/4 - (\omega_0 t)^2/3 - 7(\omega_0 t)^3/24 \right],$$

Note that for small  $t$  the change is  $\sim t^2$

For large time the mean energy in the resonance island is  $v_r^2 + V^2/4$ ,  
The energy  $\delta v_r V^2/4$  is transferred to the wave.

## Mode Particle energy transfer

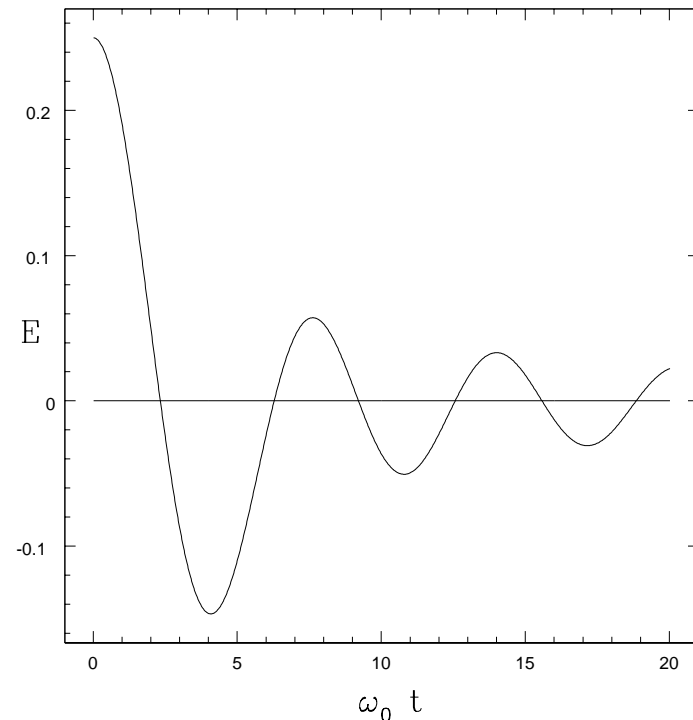
Irreversible!

The transfer of energy only happens on a time scale of  $\omega_0 t \sim 2\pi$ .

There is a delay  $\tau$  from the time of particle deposition to energy transfer to the mode, due to the finite mixing time in the resonance,

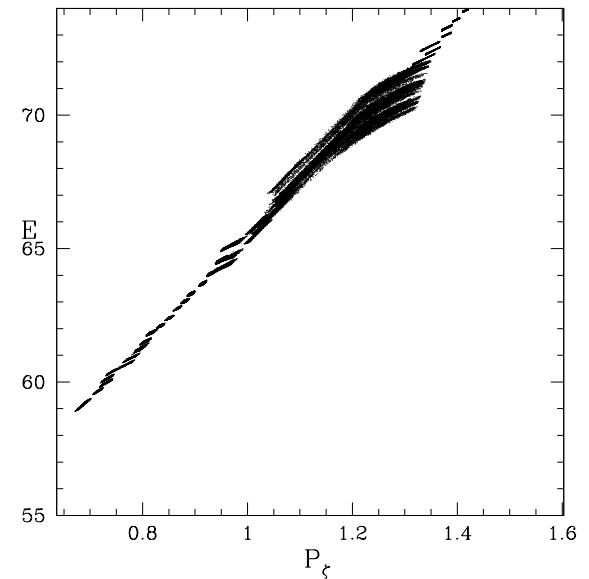
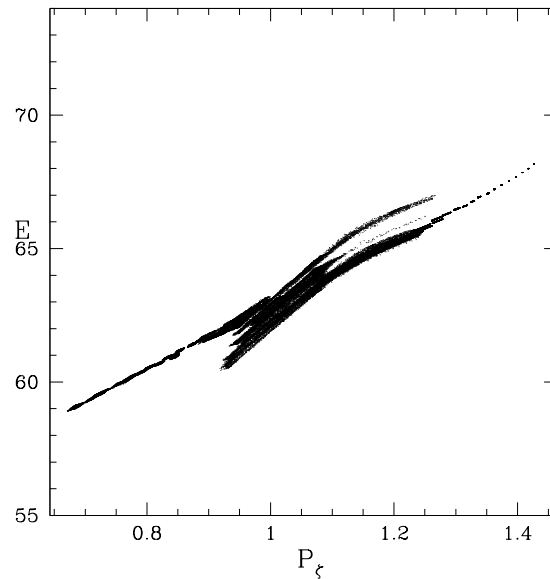
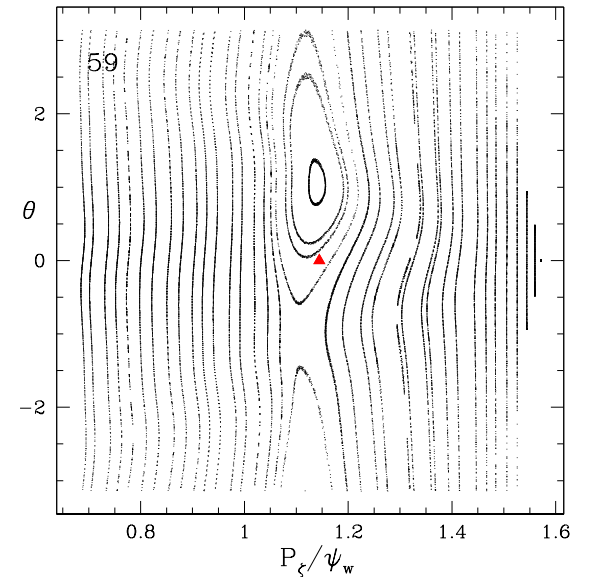
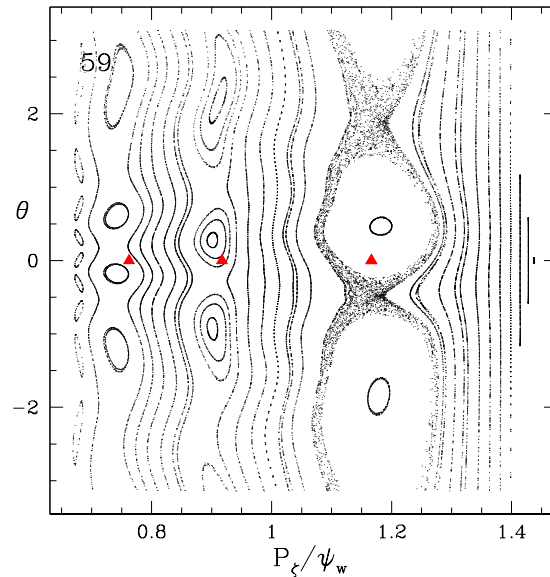
The delay is given by the period of rotation of particles in the resonance island.

The rotation frequency is an increasing function of perturbation strength, or island size, zero in the limit of zero perturbation.



# Stochastic Particle motion

Overlapping islands due to 10 kHz modes with  $m/n = 3/2$  and  $2/1$ ,  
Different  $\omega/n$  –  
Cannot see the chaos on a single plot-  
But there is chaotic transport locally in the domain where the islands overlap.  
Seen in plot of total particle motion each mode moving particles along its line of action  
 $E \sim P_\zeta \omega/n$



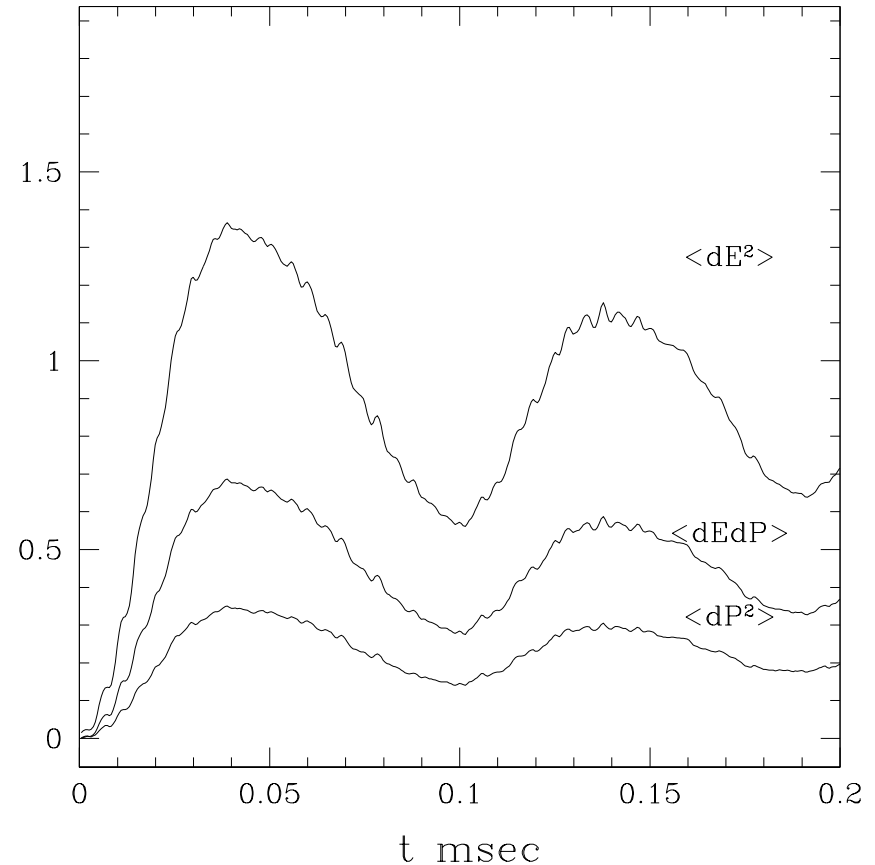
## Stochastic Particle motion

Multiple modes produce stochastic transport in limited domain where modes of different  $\omega/n$  overlap.

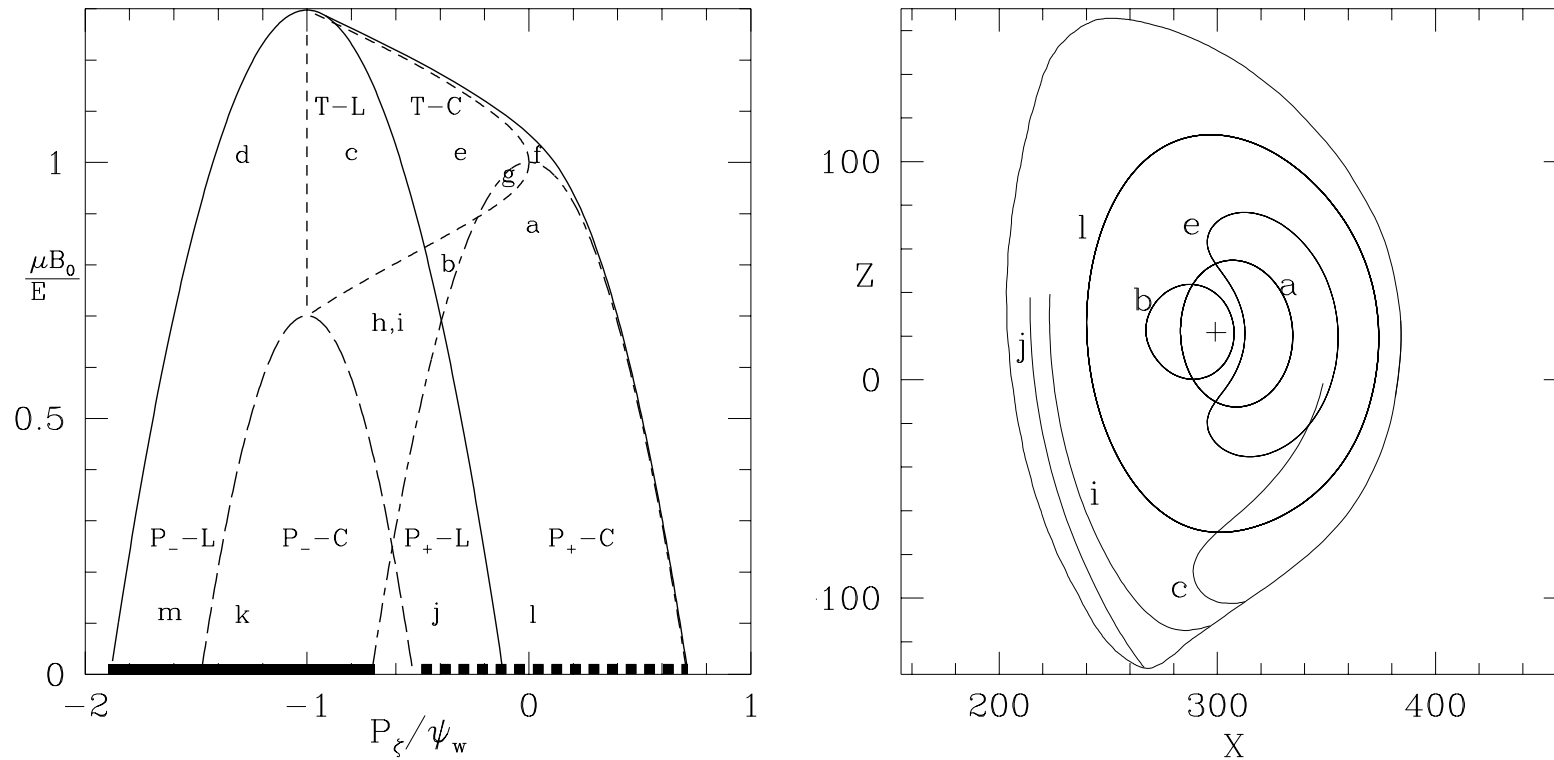
The initial linear section agrees with a quasilinear diffusion calculation

The limited domain causes particles to surge around in it until they settle down into a new configuration.

There is a secular change in the mean energy.

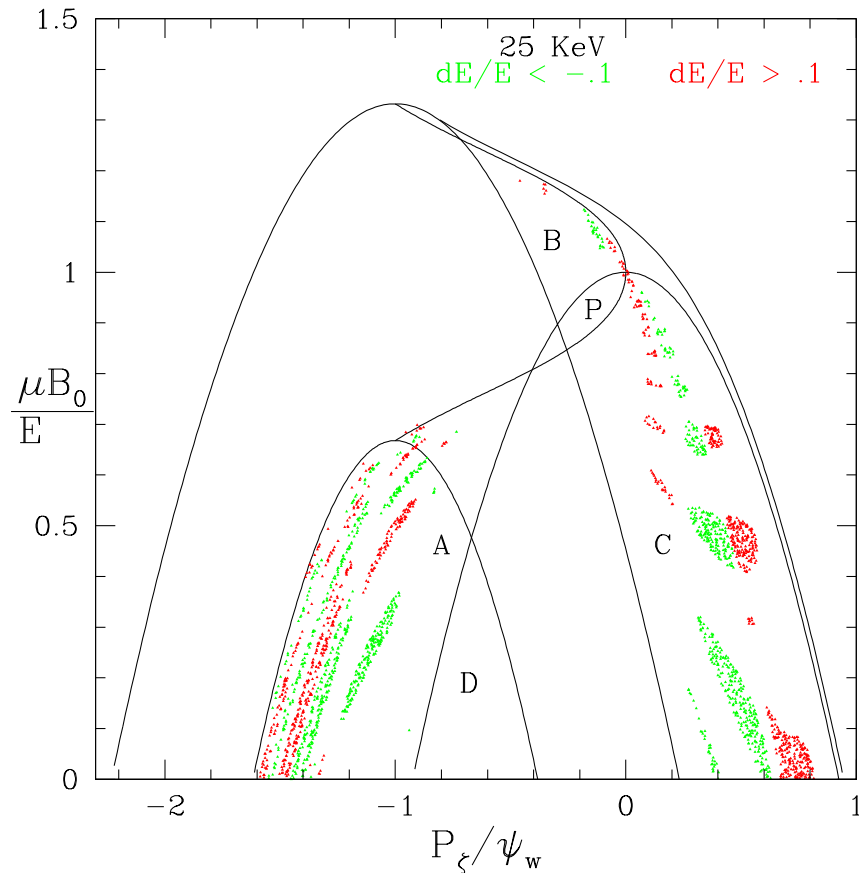


## Classification of Particle Orbits in a Tokamak, fixed $E$



Orbits determined by  $E$ ,  $P_\zeta$ , and  $\mu$ . JET equilibrium  
 For fixed  $E$  the plane of confined orbits in  $P_\zeta, \mu$  plane  
 Trapped - T, co-passing  $P_+C$ , counter passing  $P_-C$ .  
 Right wall - solid line. Left wall - long dash. Trapped passing boundary  
 - short dash, Magnetic axis - short and long dashes.

## Resonance Location by Energy exchange



A plot of the  $P_\zeta, \mu$  plane, showing only 25 keV particle orbits with energy loss or gain due to the mode, for a  $m/n = 9/2$ , mode at 90 kHz (showing 10 percent change) Must integrate over time for one Landau mixing time = O-point rotation.

Not a precise resonance location indicator, but useful.

## Classification of Particle Orbits in a Tokamak, fixed $\mu$

Since modes with frequency much smaller than the cyclotron frequency do not change  $\mu$ , the modification of the distribution occurs in the  $P_\zeta, E$  plane,

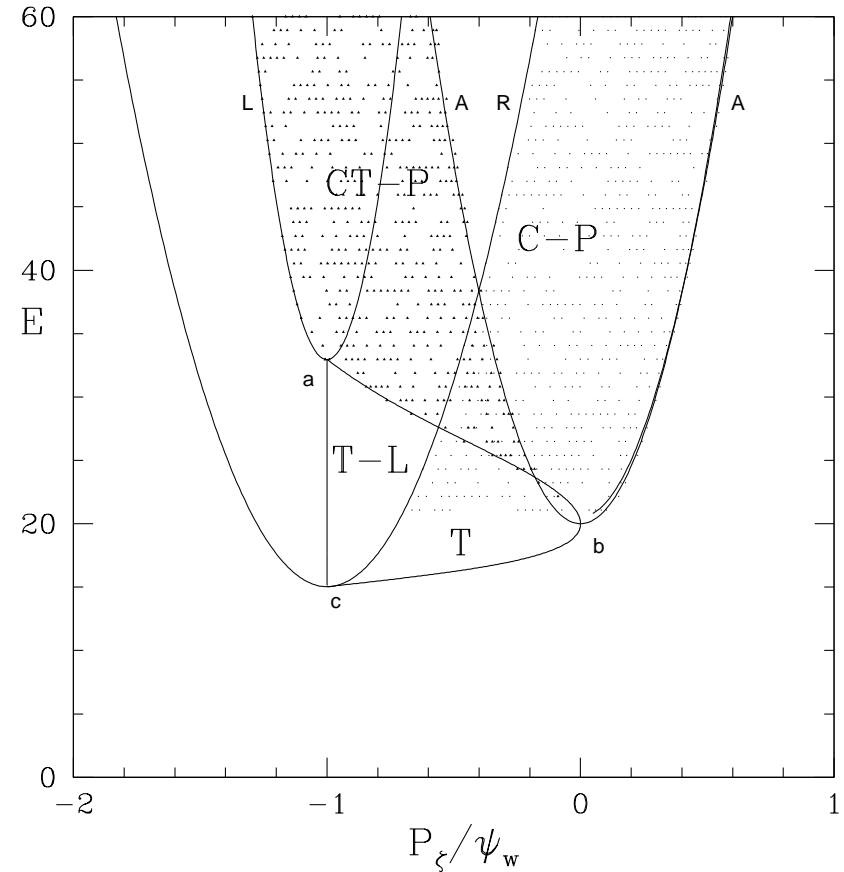
for each mode along lines

$$E - P_\zeta \omega / n = c$$

DIII-D Equilibrium with beam ion population,  $E > 20keV$

Trapped - T, co-passing C-P,  
counter passing CT-P

Magnetic Axis - A, right wall R,  
Left wall L, all parabolas.



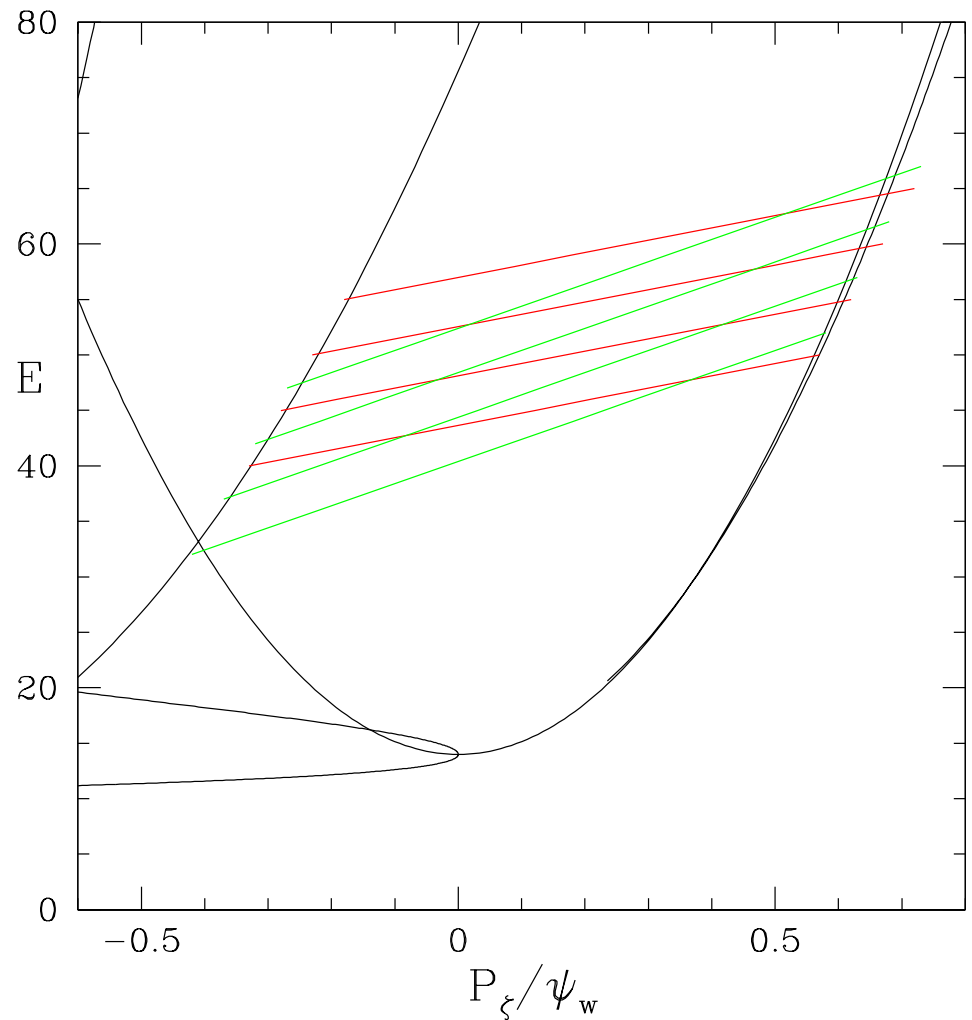
## Induced Particle motion

Each mode conserves  $\mu$  and produces motion along its line  $E - P_\zeta \omega/n = \text{const.}$

The combination of multiple modes gives stochastic transport through alternating steps due to each mode –

Lichtenberg-Lieberman,  
Stochastic Pump Model –

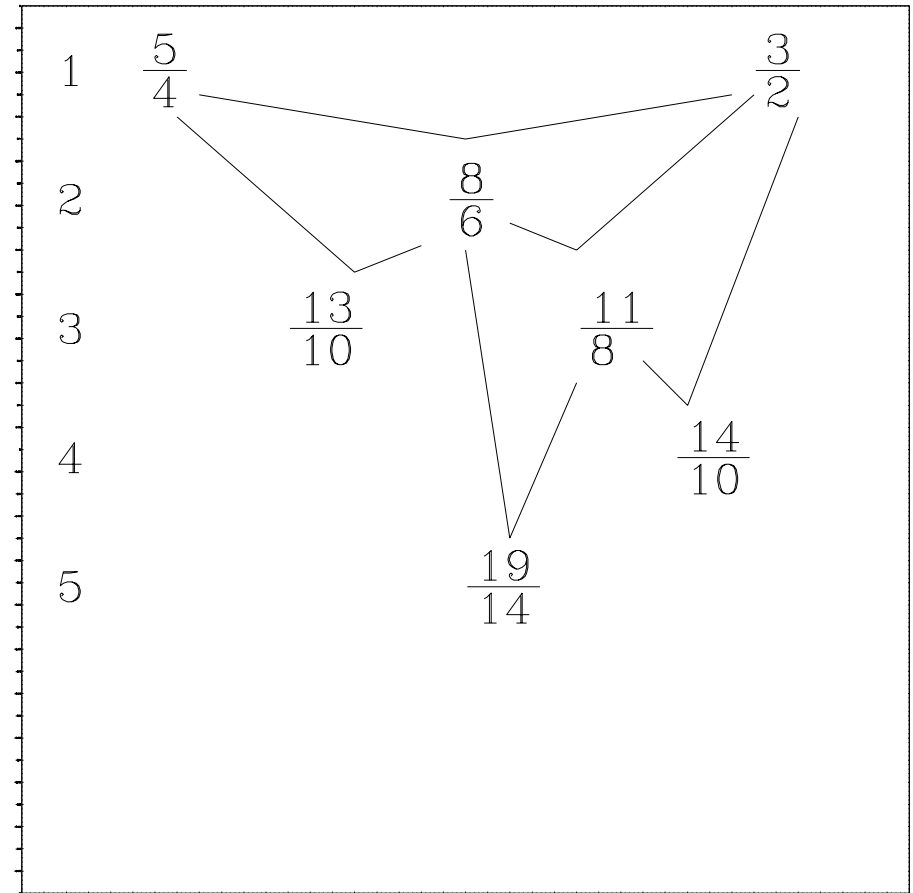
Along each line transport occurs only in domains of broken KAM surfaces for that mode, either islands or stochastic regions



## Fibonacci Sequence

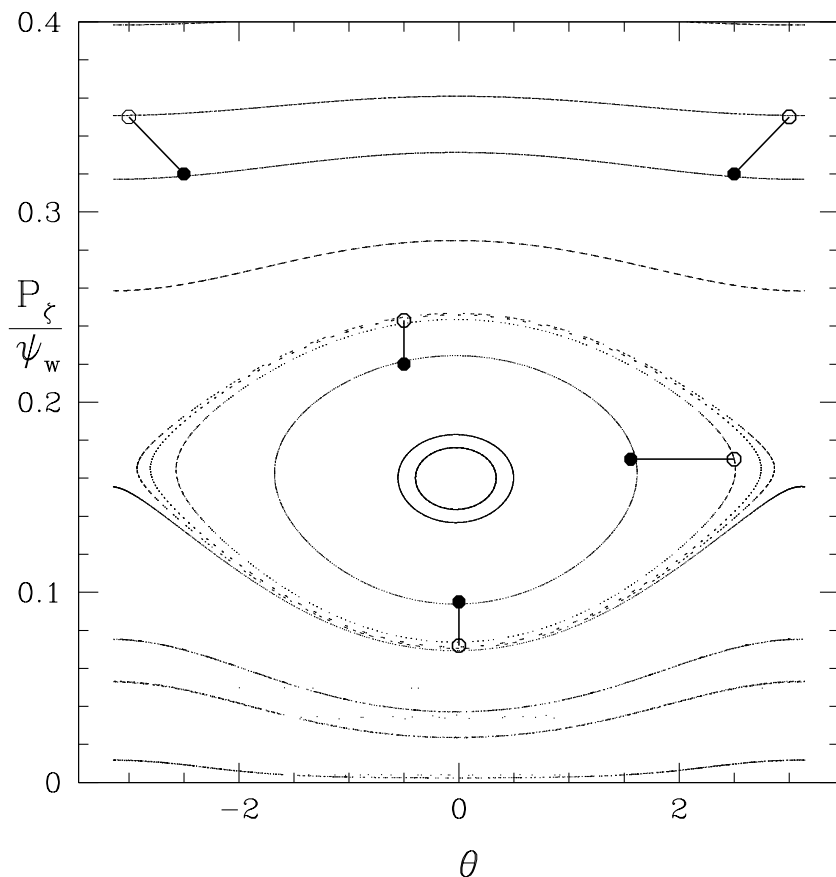
Nonlinear coupling of two modes  
 $e^{m\theta-n\zeta}$  and  $e^{k\theta-s\zeta}$   
gives  $e^{(m+k)\theta-(n+s)\zeta}$

This is a sequence of fractions  
studied by Fibonacci (1170-1250)  
Shown are a few examples with  
the perturbation order on the left.  
Note that the higher order  
fraction is always located  
in between the parent fractions.



# Determination of domains of broken KAM surfaces

Phase vector rotation — Poincare plot of  $P_\zeta, \theta$



Closely spaced pair of orbits, defining a phase vector in  $P_\zeta, \theta$  plane.

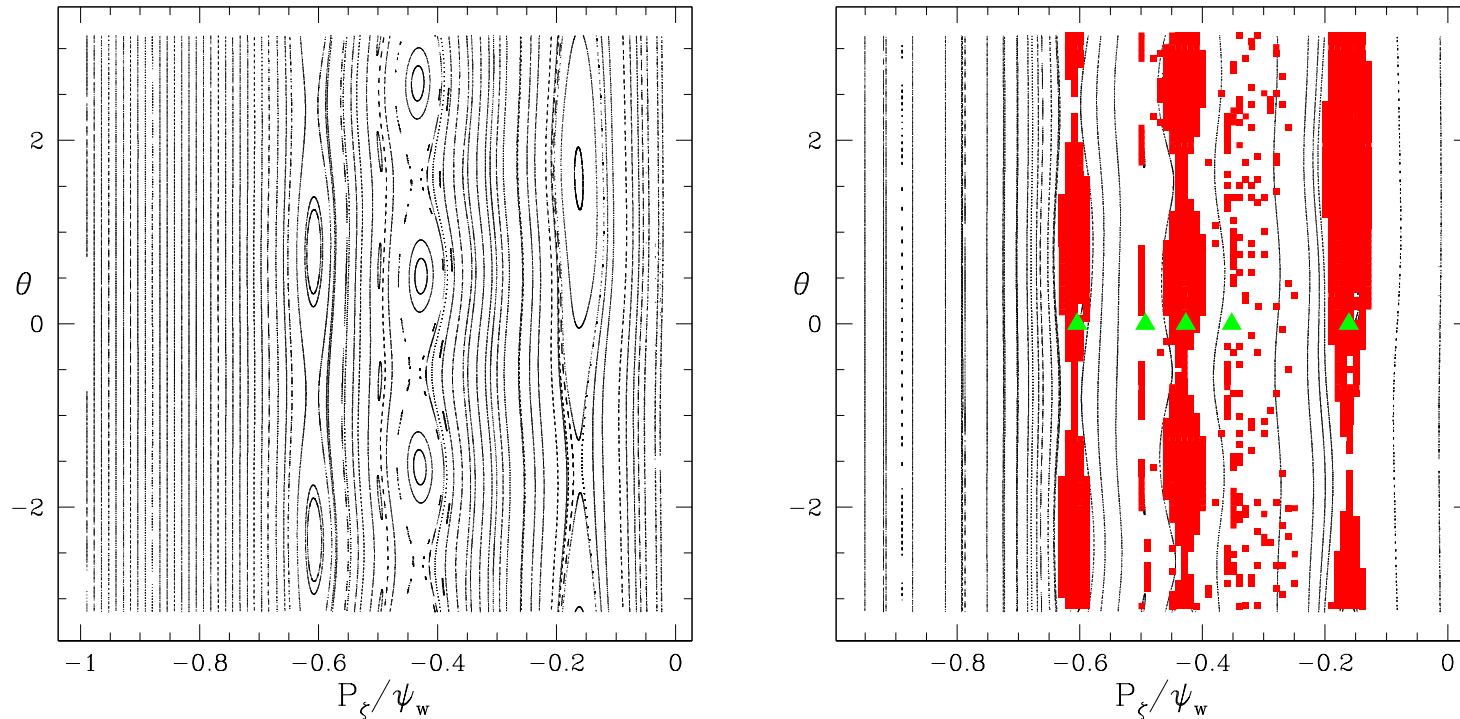
Phase vector angle  $\chi$  rotates without bound in island-internal  $q(\psi)$

Phase vector angle  $\chi$  rotation not  $> \pi$  on good KAM surfaces

**Orbit pairs can be used for diagnostic to find domains of broken KAM**

Variables advanced,  $\Delta P_\zeta, \Delta \zeta, \Delta P_\theta, \Delta \theta$

## Phase Vector island determination

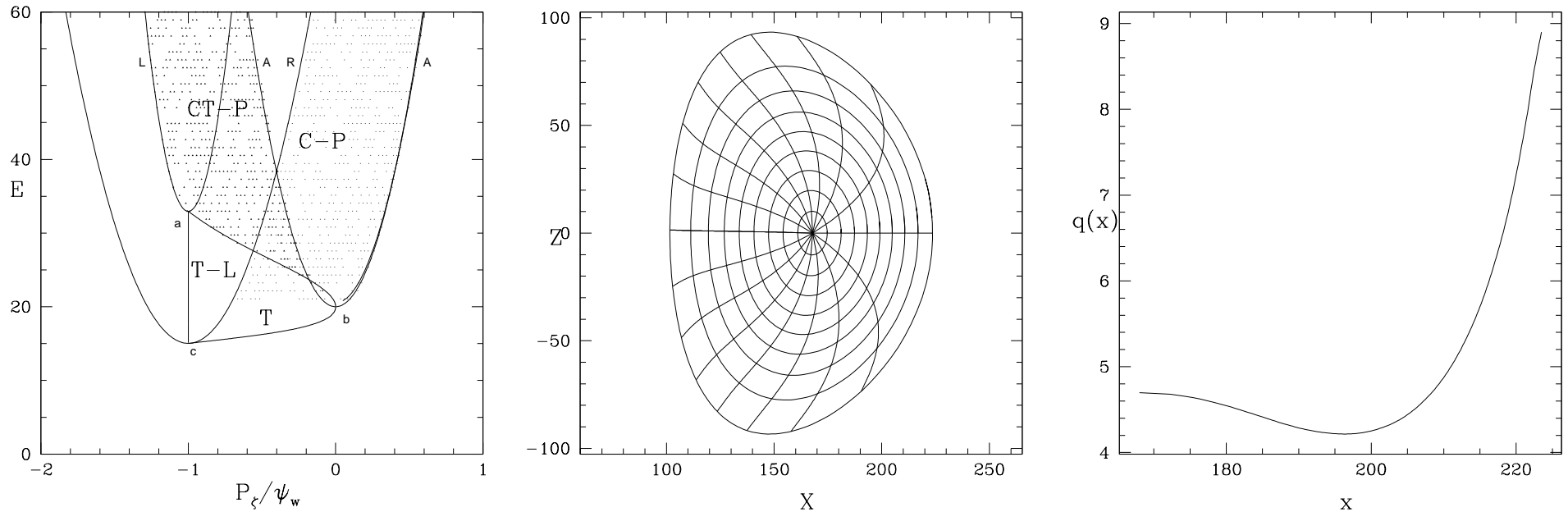


Kinetic Poincaré plot for 2/1, 3/2 and 1/1 zero frequency tearing modes, and amplitudes  $\alpha = 10^{-5}R$ , and phase vector rotation indicator.

Resonant surfaces shown with large triangles for surfaces 2/1, 5/3, 3/2, 4/3, and 1/1, listed in order as they appear from the left in the plot.

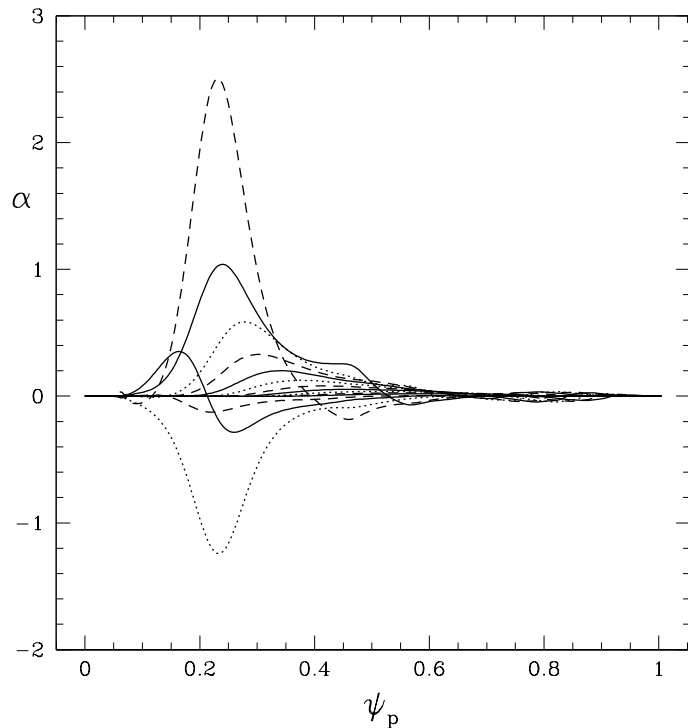
# DIII-D Reversed Shear Equilibrium

$B_0 = 20.3Kg$ , shot 122117.



Partition  $P_\zeta, E$  plane into bins  $\Delta P_\zeta, \Delta E$ , typically  $100 \times 100$  bins  
Launch orbit pairs in all bins in confined domains  
For each bin find whether orbits belong to good KAM or not

## Harmonic content of one DIII-D TAE mode at 81 kHz



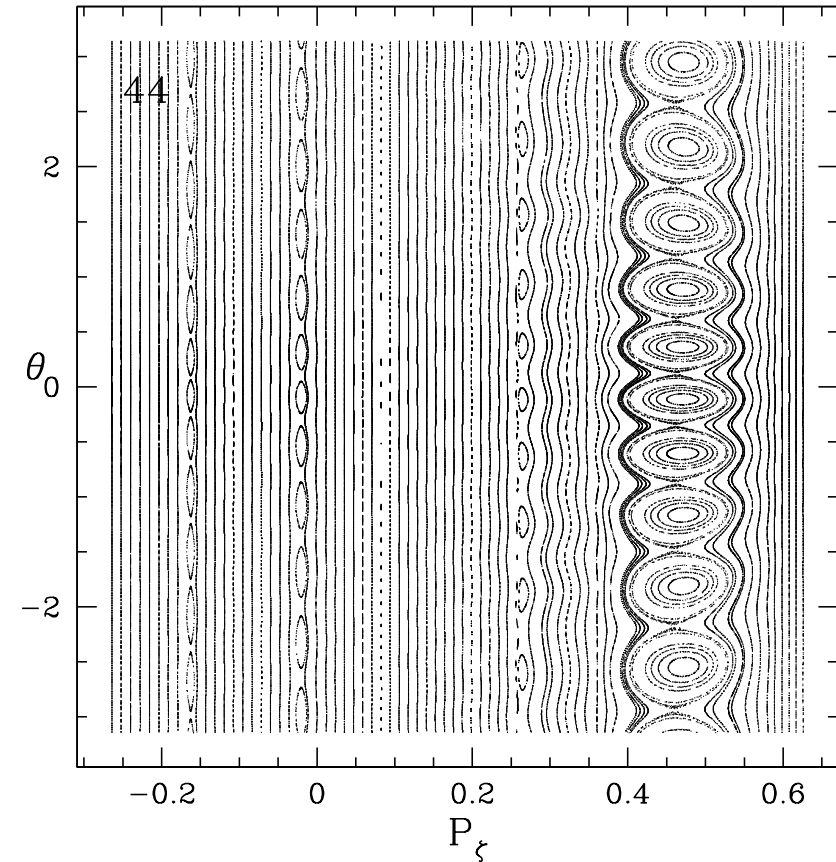
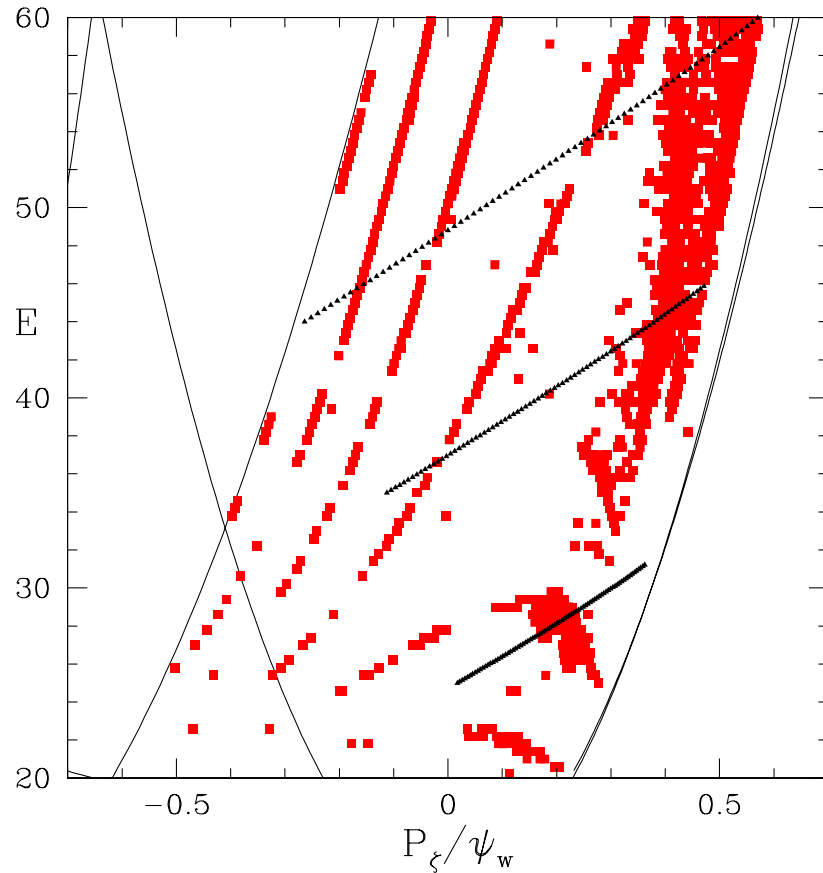
$n = 3, 10 \leq m \leq 23,$   
Typically each TAE mode has 10-12 poloidal harmonics  
Eleven different modes present in shot 122117, total of 151 harmonics.  
Most modes localized near plasma center

## Phase Vector Rotation Method Confirmation

Distribution space divided into 12 domains of  $\mu B$

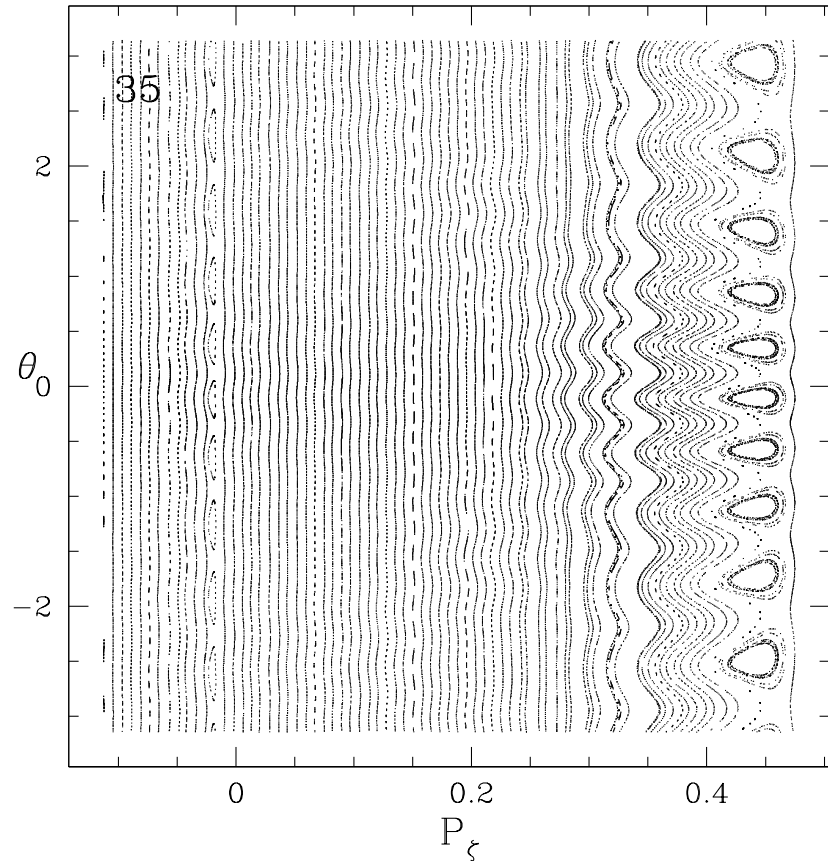
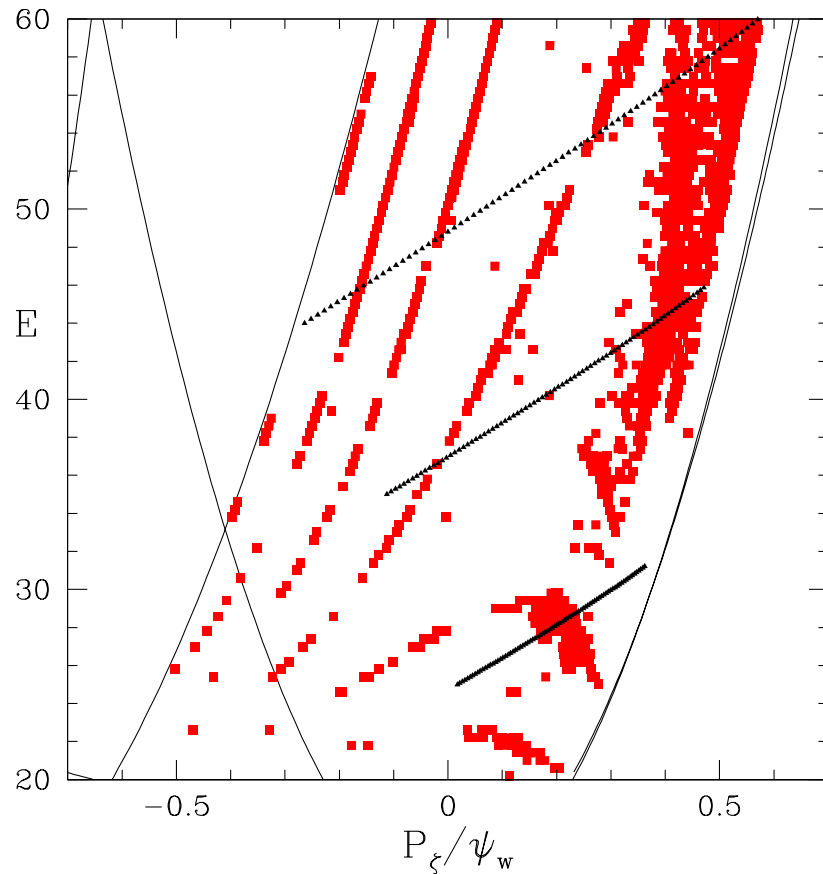
For each value of  $\mu B$  the  $P_\zeta, E$  plane sectioned into 100 X 100 domains

A few orbit pairs launched in each domain with different values of  $\zeta$ .



$P_\zeta, E$  plane,  $\mu B = 14KeV$  broken KAM and Kinetic Poincaré - 81 kHz mode  $n = 3$  Kinetic Poincaré starting at 44 keV, shows  $m'/n = 12/3, 11/3, 10/3$  resonances.

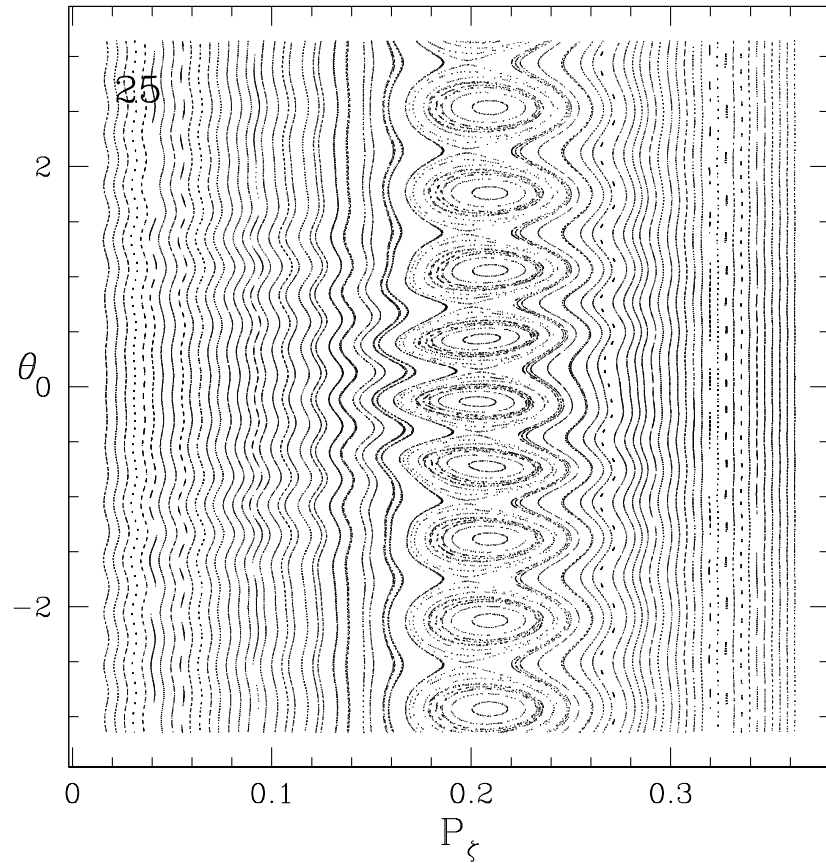
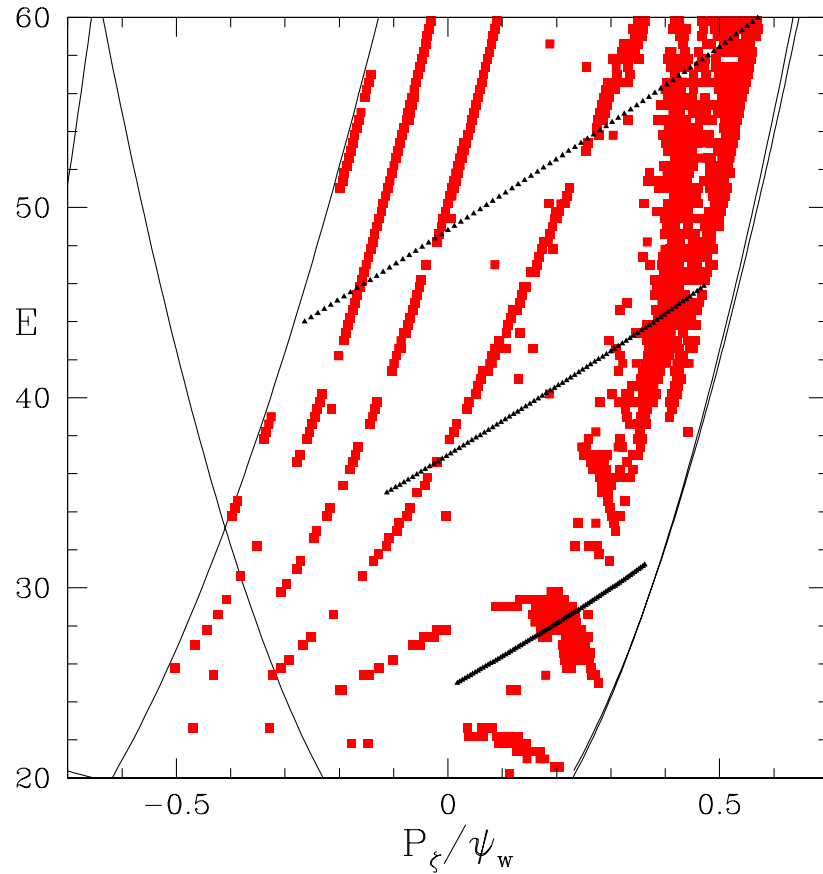
## Phase Vector Rotation Confirmation



$P_\zeta, E$  plane,  $\mu B = 14KeV$  broken KAM and Kinetic Poincaré - 81 kHz mode  $n = 3$

Kinetic Poincaré starting at 35 keV shows the same small ten island resonance seen in the first plot, now at  $P_\zeta = -0.02$ , and the same large ten island resonance now at  $P_\zeta = 0.45$ .

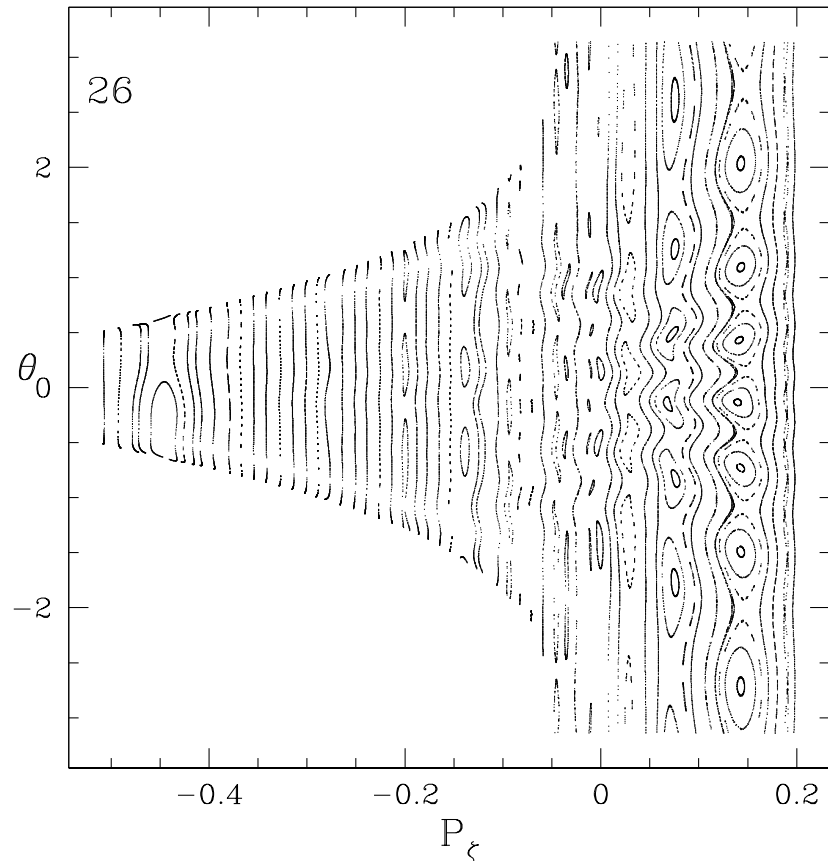
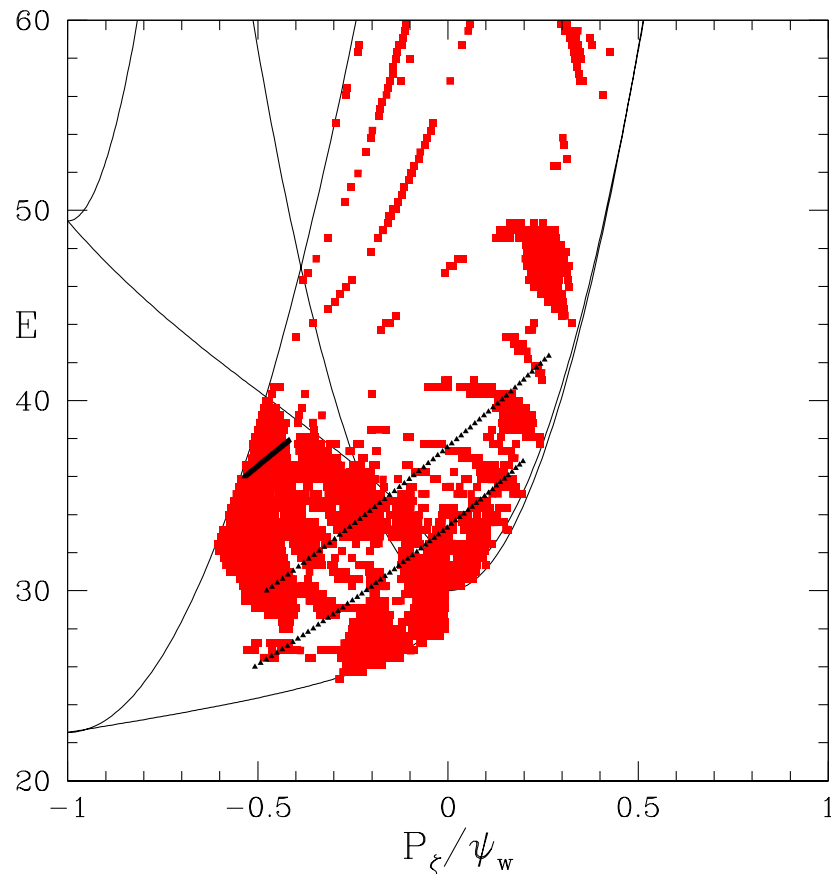
## Phase Vector Rotation Confirmation



$P_\zeta, E$  plane,  $\mu B = 14KeV$  broken KAM and Kinetic Poincaré - 81 kHz mode  $n = 3$

Kinetic Poincaré starting at 25 keV, shows a large nine island resonance at  $P_\zeta = 0.21$ .

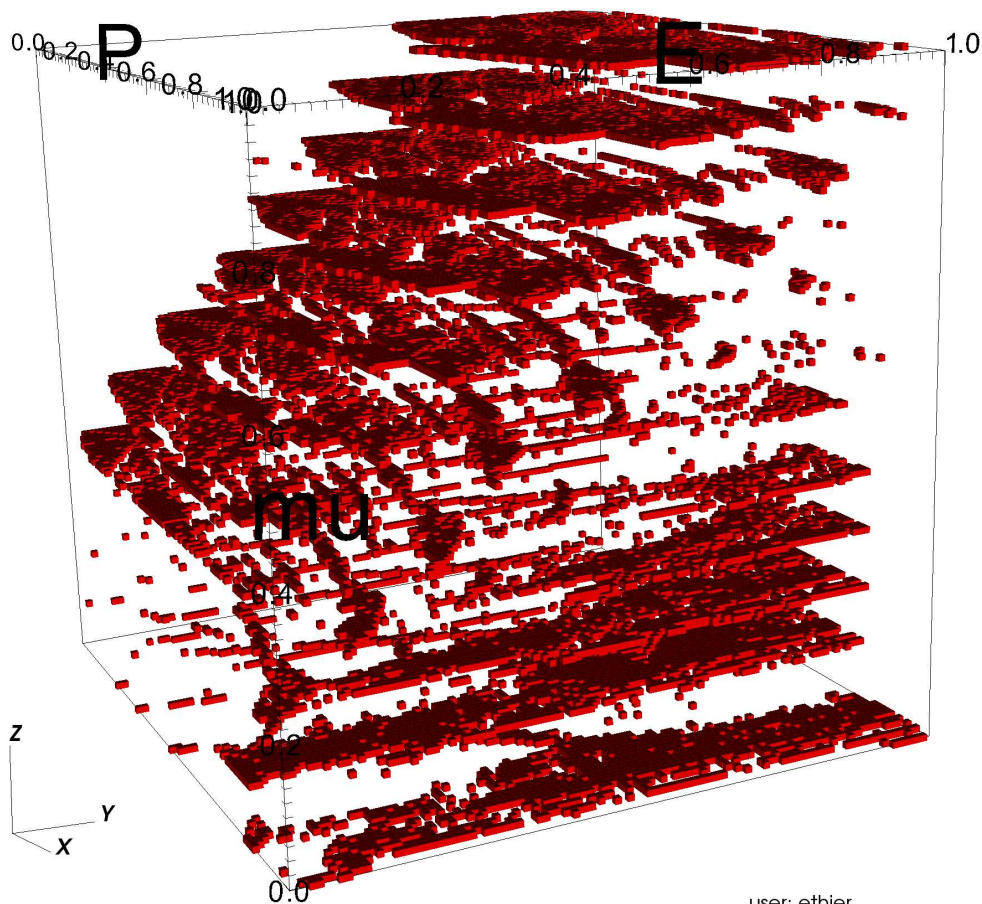
## Phase Vector Rotation Confirmation



$P_\zeta, E$  plane  $\mu B = 30KeV$  broken KAM and Kinetic Poincaré - 81 kHz mode  $n = 3$   
Kinetic Poincaré for the line starting at 26 keV, shows a  $m' = 1$  resonance at  $P_\zeta = -0.45$  and many small resonances near the trapped passing boundary  
**Phase vector rotation gives exact information about resonance location and width, subject only to the resolution determined by density of points and time**

DB: solid\_hires.3D  
Cycle: 0

Scatter  
Var: P,  
E,  
mu

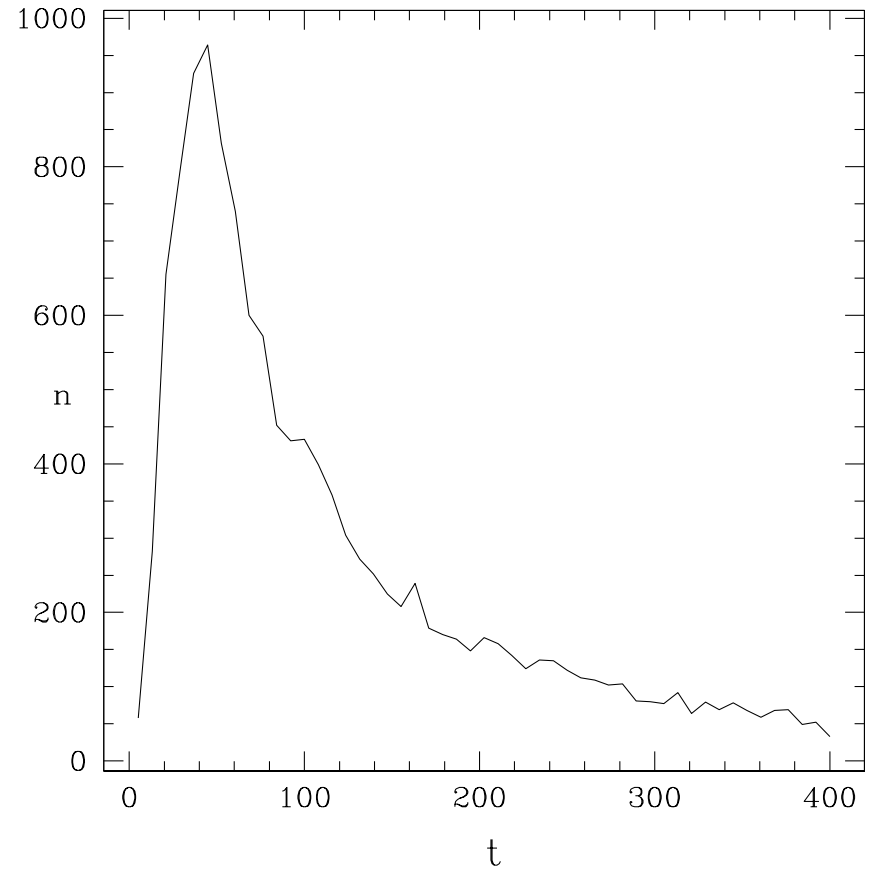
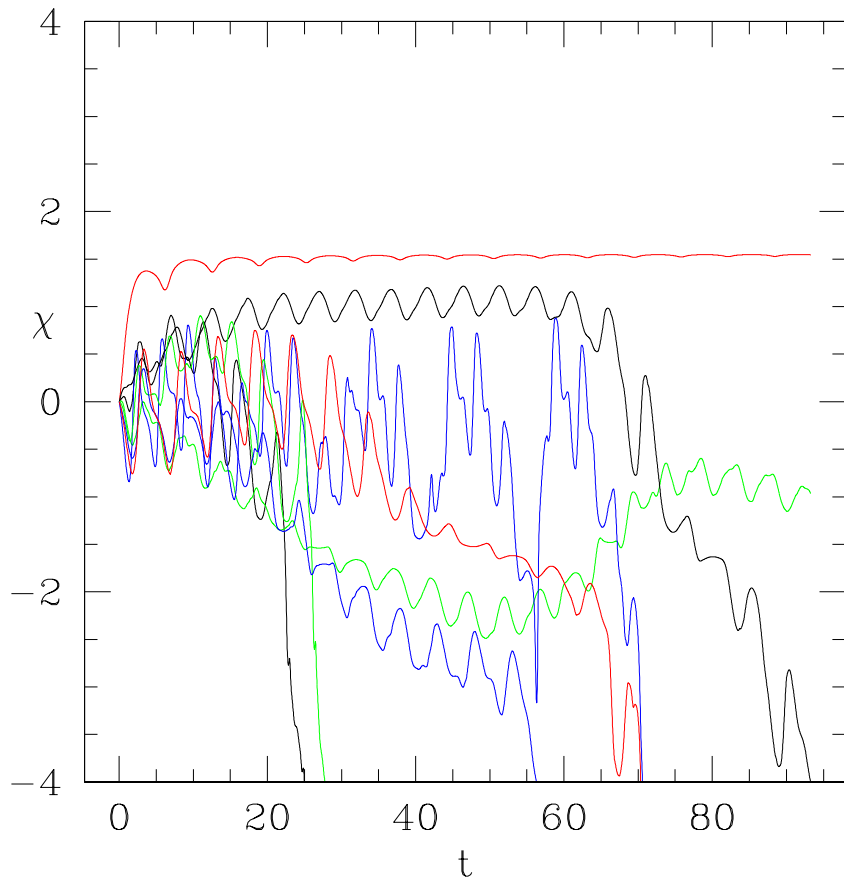


user: ethier  
Tue Jan 11 11:08:53 2011

Resonances in DIII-D  
for an 81 kHz  $n = 3$   
mode in the  $P_\zeta$ ,  $E$ ,  $\mu$   
volume

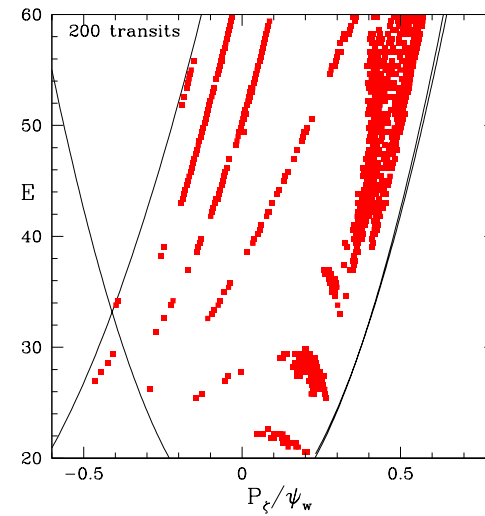
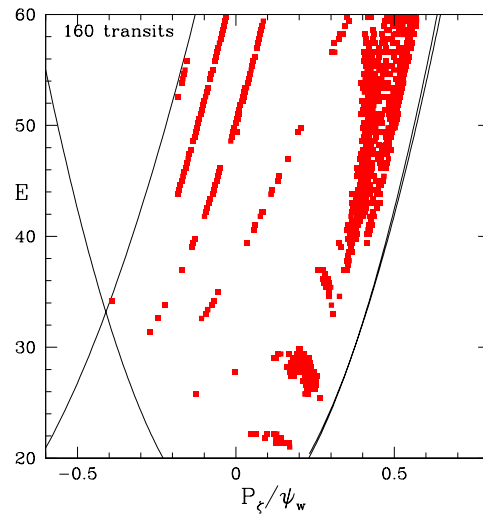
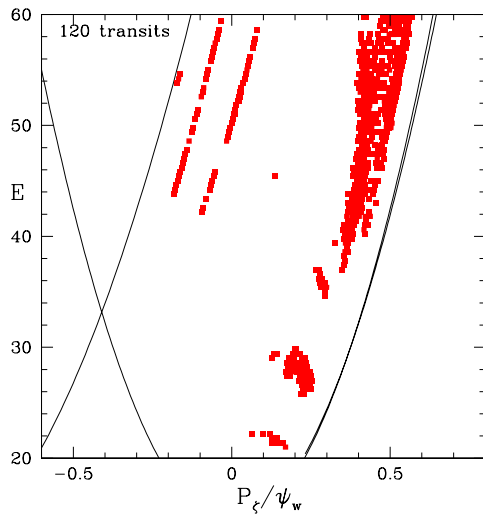
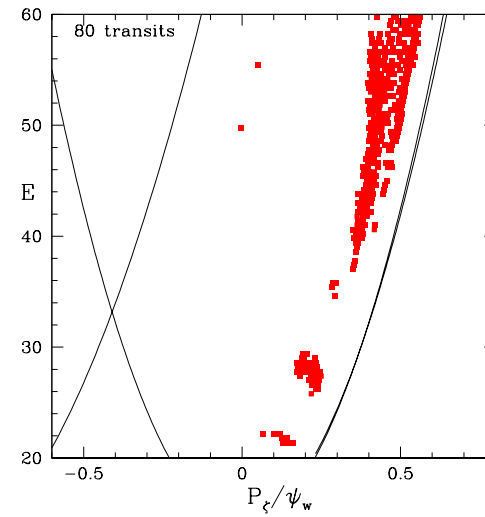
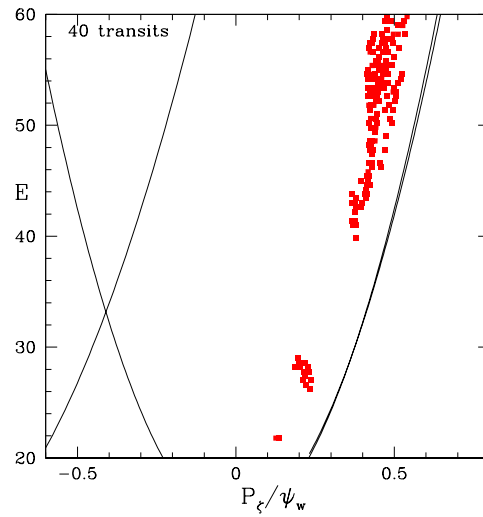
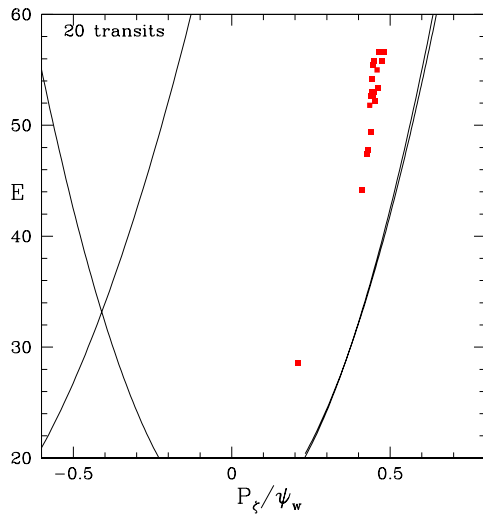
Space is left between  
values of  $\mu$  to allow  
visualization.

Each mode produces  
many small islands but  
no stochastic domains.  
Usual search of finding  
chaos by looking for last  
broken KAM surface is  
not the right problem to  
solve.



Time history of  $\chi$  for some orbit pairs, and histogram of time (transits) required to reach  $\chi = 4$ . It has been verified that  $\Delta P_\zeta$ ,  $\Delta \psi_p$ ,  $\Delta \theta$ ,  $\Delta \zeta$  remain small over whole history making a differential analysis possible -  $\Delta \zeta$  is oscillatory, complicates the Poincaré picture

Large Islands appear first, followed by small resonances



## Evolution of Particle Distribution

### Annealing of adjacent stochastic domains

Volume occupied by orbit shell with  $dP_\zeta$

$$dV \sim dP_\zeta \int d\theta \left( \frac{d\psi_p}{dP_\zeta} \right)_{E,\mu} J(\psi_p, \theta),$$

integration over the particle orbit.

$$dV = dP_\zeta \int d\theta \frac{(gq + I)}{B^2} \frac{1}{1 + g(\rho_{\parallel}^2 B + \mu) \partial_{\psi_p} B / \rho_{\parallel} B^2 - g' \rho_{\parallel}}$$

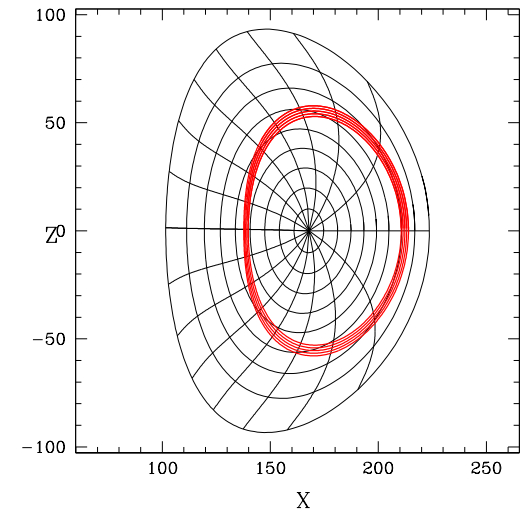
In neighboring stochastic domains along the lines with  $E - P_\zeta \omega / n = c$

initial particle numbers in the domains  $n_1, n_2$  and  $n_1 + n_2 = N$

Particle conservation  $n'_1 + n'_2 = N$ , Equal densities  $n'_1 / dV_1 = n'_2 / dV_2$

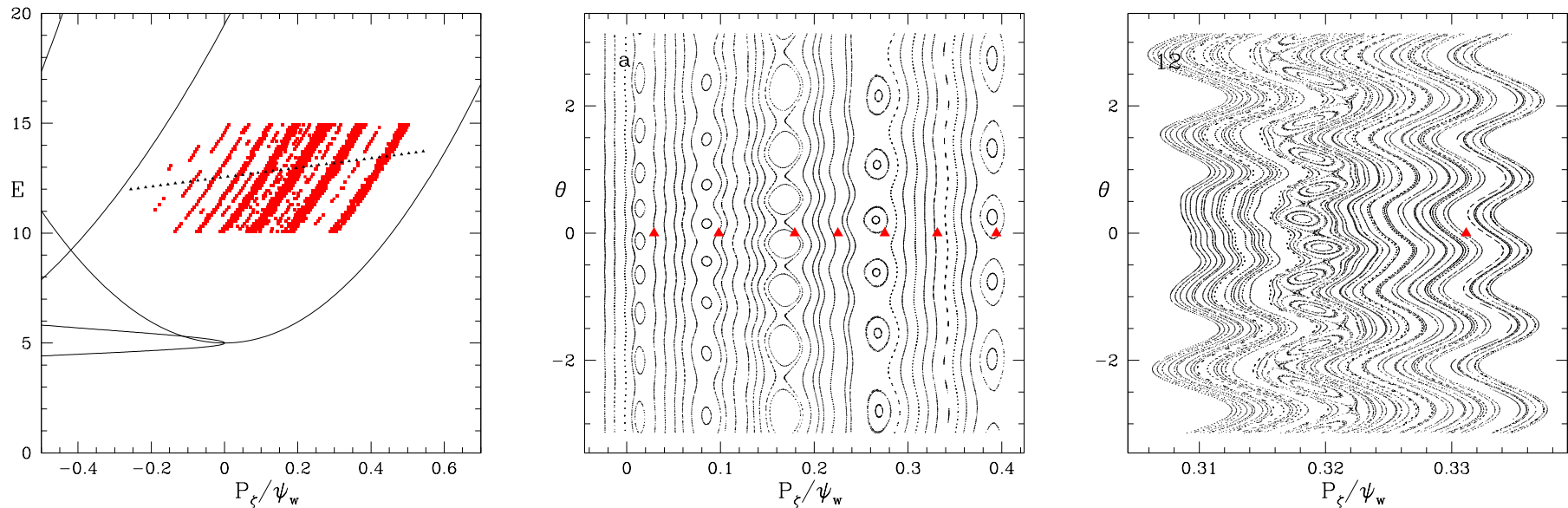
$$n'_1 = \frac{N dV_1}{dV_1 + dV_2}, \quad n'_2 = \frac{N dV_2}{dV_1 + dV_2}.$$

**Each annealing iteration corresponds to a diffusion step by  $\Delta P_\zeta$ .**



## Broad low amplitude $m/n = 6/5$ mode, Phase Vector plot

Primary resonances and first order Fibonacci resonances (1170-1250)



Circular Equilibrium  $.8 < q < 4$  ,  $R = 100cm$  ,  $a = 25cm$  ,  $B = 20kG$

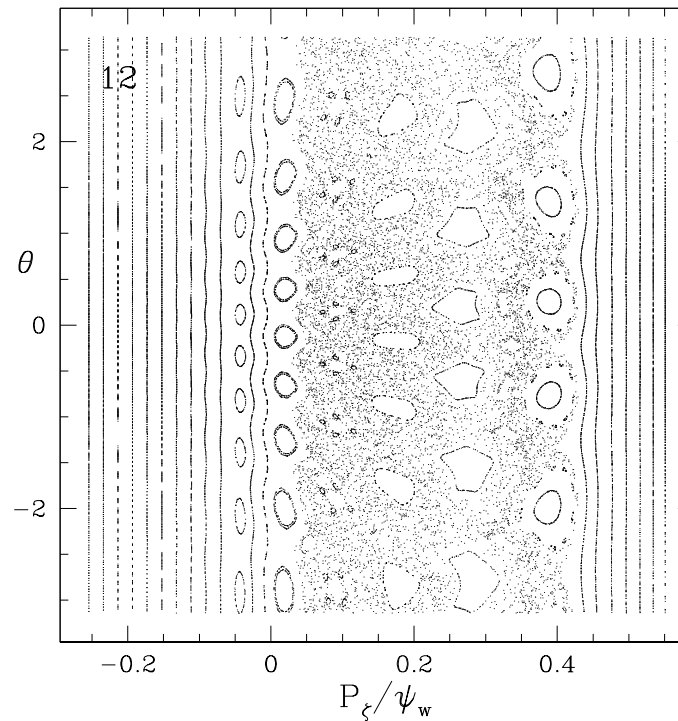
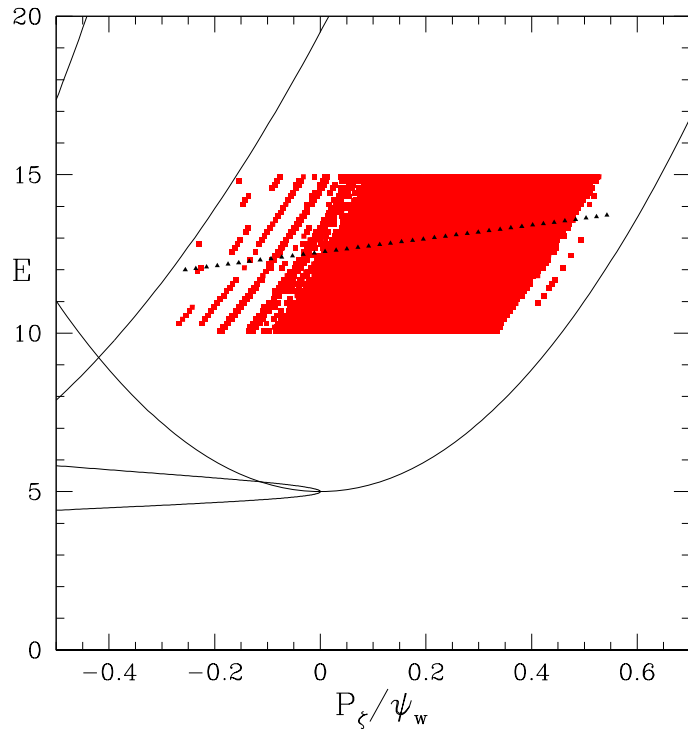
$P_\zeta, E$  plane  $\mu B = 5KeV$  - **10 kHz mode  $m/n = 6/5$  and  $\alpha = 5 \times 10^{-6}R$**

Kinetic Poincaré showing resonances at  $m'/n = 9/5, 8/5, 7/5, 6/5, 5/5$

First Fibonacci resonance 11/10. **Triangles show analytic Resonance surfaces.**

**Avalanche due to broad large amplitude  $m/n = 6/5$  mode —**  
 Annealing takes place along lines  $E - P_\zeta \omega/n = c$  if adjacent domains are chaotic.

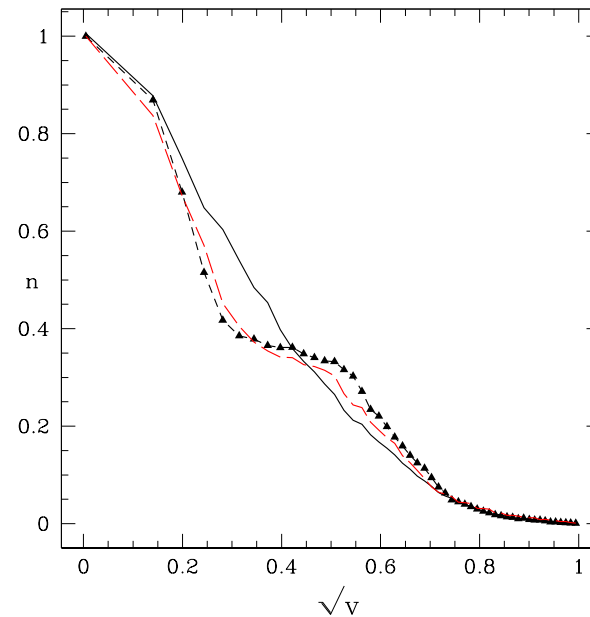
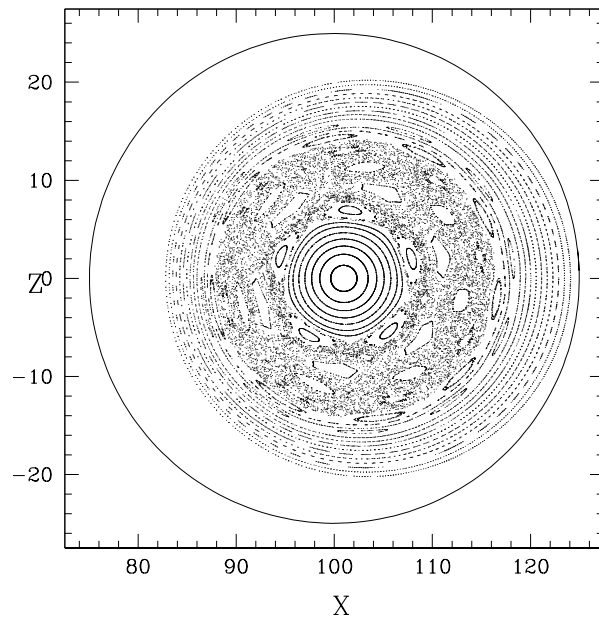
**Each annealing iteration corresponds to a diffusion step by  $\Delta P_\zeta$ .**



**$P_\zeta, E$  plane  $\mu B = 5KeV$  broken KAM domains and Kinetic Poincaré plot**  
**10 kHz mode  $m/n = 6/5$  and  $\alpha = 5 \times 10^{-5} R$**   
 One hundred domains in  $P_\zeta$  and fifty in  $E$ .

## Result of annealing, large amplitude $m/n = 6/5$ mode

Annealing takes minutes of computing time for hundreds of iterations

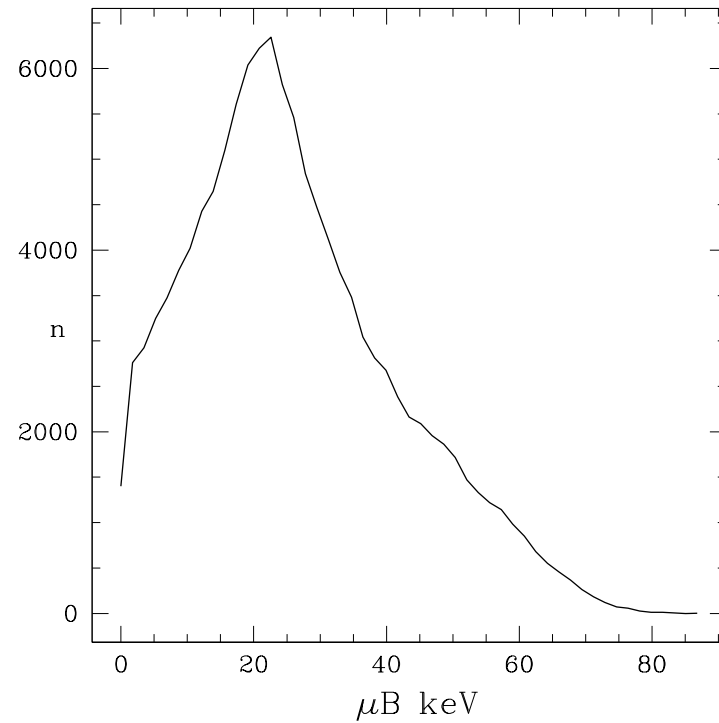
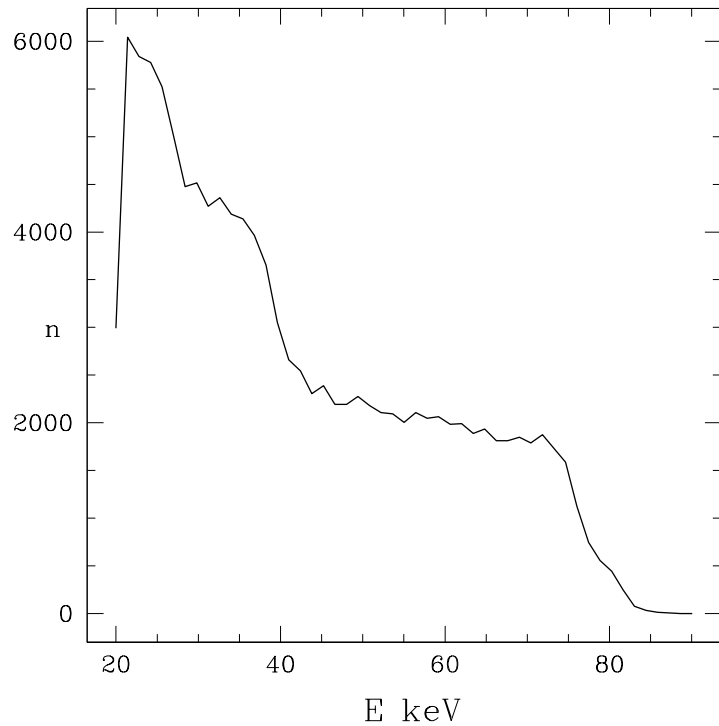


**Kinetic Poincaré in X,Z plane - 10 kHz mode  $m/n = 6/5$**

**Simple distribution with  $\mu B = 5KeV$ ,  $10 < E < 15$  and radial profile**

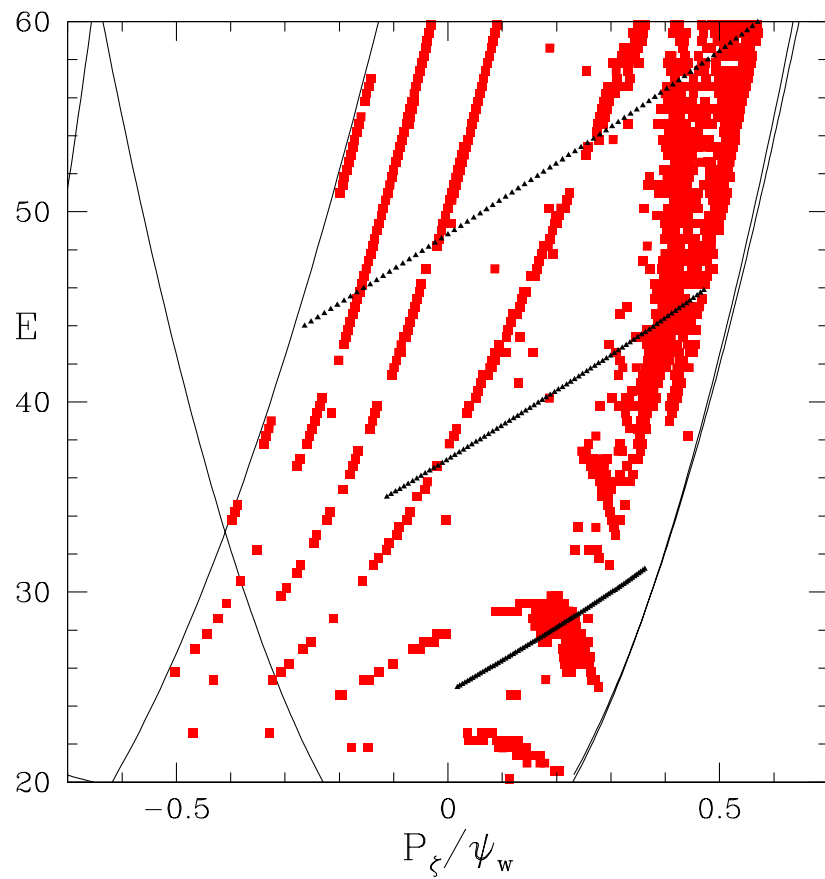
**Annealing due to hundreds of iterations and result of Guiding Center simulation**

## DIII-D Distribution from beam deposition code TRANSP



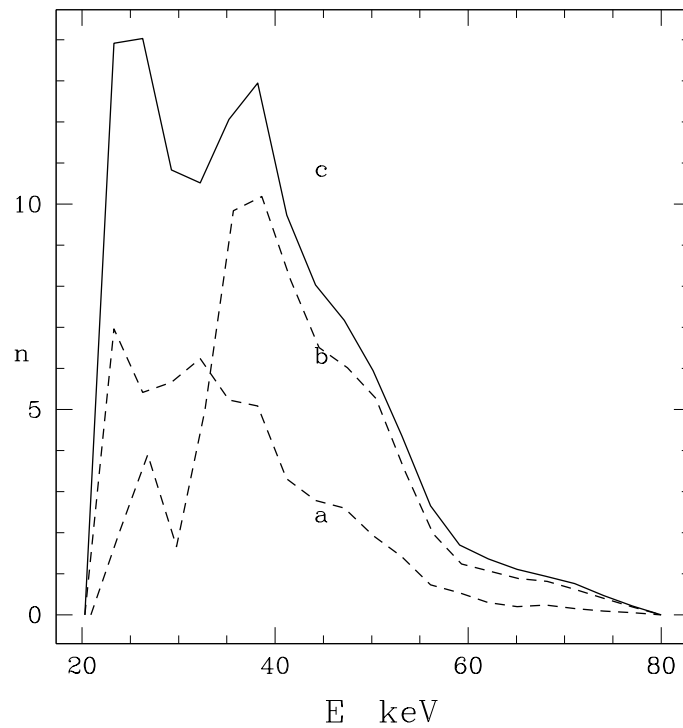
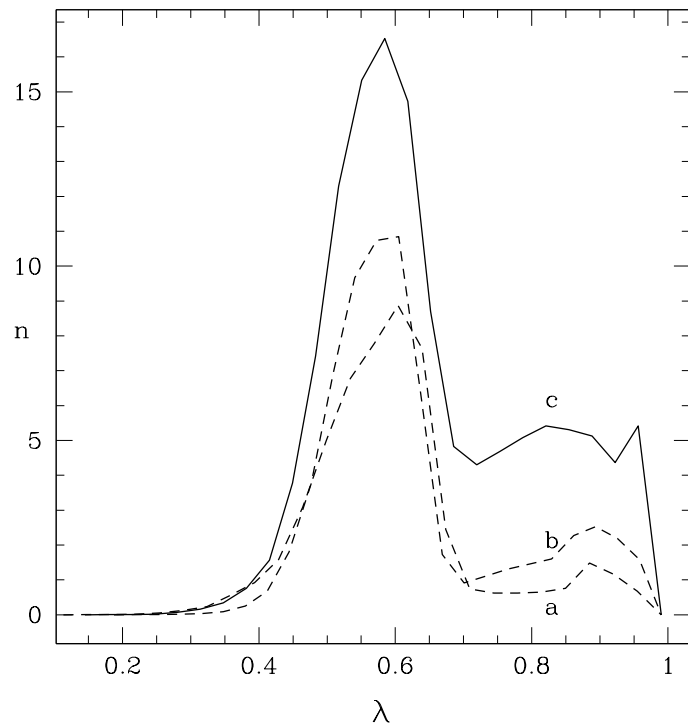
Beam consists of mostly co-passing particles. 12 domains in  $\mu$   
Particles loaded and then annealing process for all 11 modes applied.  
Each iteration is diffusion step in  $\Delta P_\zeta$  with time given by quasilinear value, in this case about 0.1 msec for each step  $\Delta P_\zeta$ .

For each value of  $\mu$  annealing is carried out, one mode at a time. Each mode moves particles along its line  $E - P_\zeta \omega/n = c$ . Only where KAM surfaces are broken. The combination of the modes leads to stochastic particle motion in the  $E, P_\zeta$  plane and can lead to profile flattening and loss.

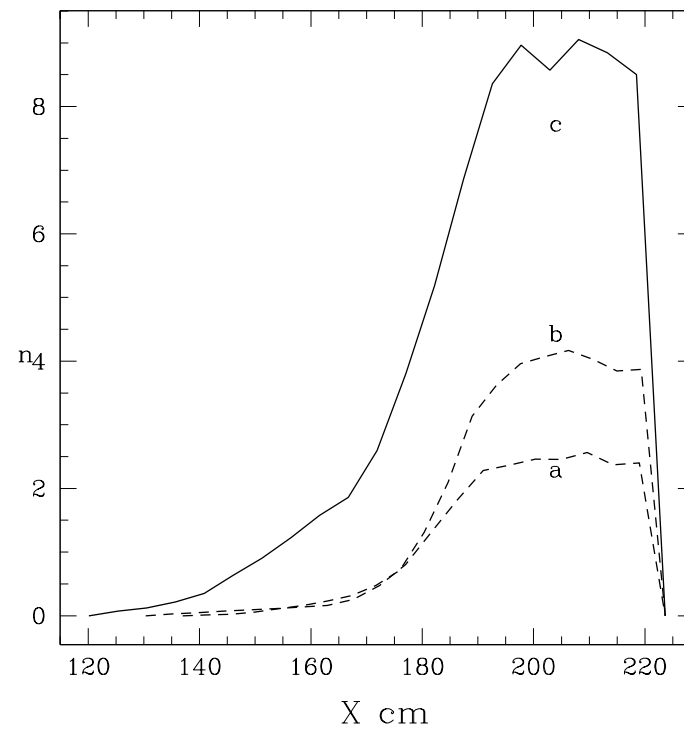
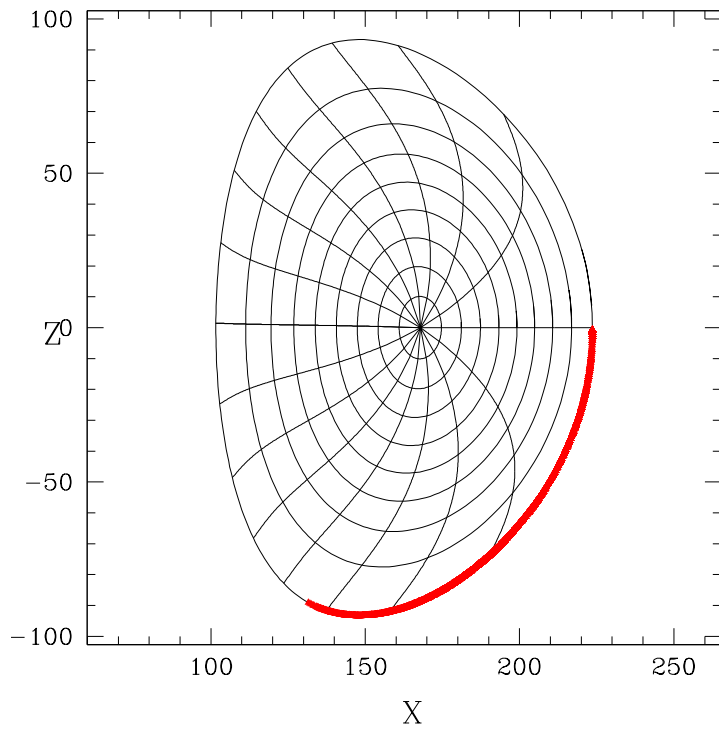


For the DIII-D case there were 11 TAE modes, and for each mode one must do the annealing for each  $\mu$  value. After the annealing is done the particle distribution is reconstructed. Particles in chaotic domains near the last closed flux surface are lost. Each annealing iteration moves particles the width of one domain  $\Delta P_\zeta$ . Even for hundreds of annealing steps this computing is negligible.

**DIII-D Loss, with  $dB/B =$  (a)  $2 \times 10^{-4}$  (b)  $3 \times 10^{-4}$  (c)  $4 \times 10^{-4}$**   
Distribution in pitch and energy of loss caused by modes

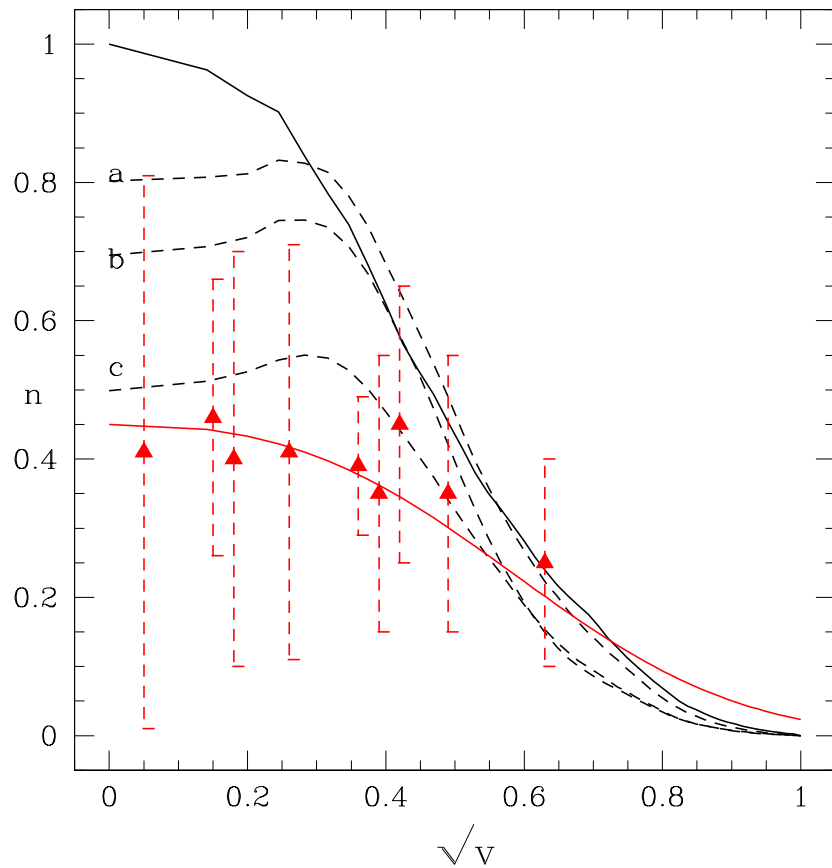


**DIID-D Loss, with  $\text{dB}/\mathbf{B} =$  (a)  $2 \times 10^{-4}$  (b)  $3 \times 10^{-4}$  (c)  $4 \times 10^{-4}$**   
Distribution on outer wall of loss caused by modes



**DIII-D - Distribution with  $dB/B = 2, 3, 4 \times 10^{-4}$  after 60 msec, and experimental points, showing clear threshold.**

Non KAM domains- each mode 30,000 particles 100 transits= 0.1 msec  
One mode annealed at a time, cycle through modes over and over  
Full guiding center simulations followed 20,000 particles for 60 msec



Resonance locations and island widths can be estimated analytically but only inexactly.

New method for determination of domains of broken KAM surfaces in the space of  $P_\zeta$ ,  $E$ ,  $\mu$  describing confined particles in a toroidal confinement device due to the presence of a spectrum of MHD modes.

The method was applied to a previously studied and well documented case of toroidal Alfvén modes in the DIII-D tokamak.

This method gives a clear detailed understanding of the effect of each mode on the particle distribution, and shows which modes produce losses as well as what part of the distribution is lost. It also reasonably reproduces the main results of a full guiding center simulation, and gives the possibility of rapid evaluation of particle loss.

The present method requires orders of magnitude less computing than a full guiding center simulation.

The present analysis must be understood to give the initial response of a distribution to a spectrum of modes, not a long time simulation of the coupled system.

After significant modification of the distribution the mode spectrum will change, so it does not make sense to continue this process once the distribution is modified.

However it gives a means of quickly examining a given particle distribution and mode spectrum to understand whether profile modification would occur.

In addition, it is not difficult to imagine for the future an iteration involving the calculation of instabilities produced by a given equilibrium, the evolution of the distribution due to the modes using this method, and a return to calculation of the modified instability spectrum.